LUNDS UNIVERSITET

DEPARTMENT of PSYCHOLOGY

Regional atrophy correlates of domain-specific episodic memory in early Alzheimer's disease

Hannah Baumeister

Master's Thesis (30 hp)
Spring 2021

Supervisor: Mikael Johansson

Abstract

Alzheimer's disease (AD) is characterized by amyloid-β (Aβ) and tau depositions as well as neurodegeneration, and is typically accompanied by a progressive decline in episodic memory. Previous research proposes two neural memory networks that process different stimulus domains. Specifically, a posterior-medial (PM) and an anterior-lateral (AL) network handle scene- and object-specific information, respectively. I aimed to determine if scene- and object-based memory follow different trajectories in early AD stages. Moreover, I tested where on the AD continuum first alterations in measures of regional atrophy occur. Finally, it was assessed if AD proteinopathy and regional atrophy are related to markers of domain-specific episodic memory. In a sample of $N = 121$ older adults who were cognitively unimpaired (CU) and Aβ negative (CU Aβ-), CU and Aβ positive (CU Aβ+), or had AD-related mild cognitive impairment (MCI Aβ+), regional atrophy measures were obtained using structural magnetic resonance imaging. Aβ and tau burden were quantified using positron emission tomography. Participants completed a mnemonic discrimination task targeting object- and scene-based episodic memory. Analyses of covariance revealed significantly smaller cornu ammonis 2/3 gray matter volumes and a trend towards lower object discrimination in the MCI Aβ+ group compared to both CU groups. In the whole sample, regression models showed that early tau burden was negatively related to object discrimination. Earliest AD-related memory decline might initially affect object-processing memory networks and is possibly driven by tau. Neurodegeneration might not mediate the relationship of AD proteinopathy and cognition until later AD stages.

Keywords: Alzheimer's disease, episodic memory, amyloid-β, tau, atrophy, neurodegeneration, mnemonic discrimination, response bias

Introduction

Alzheimer's disease (AD) is a neurodegenerative disease characterised by depositions of amyloid-β (Aβ) plaques and neurofibrillary tangles of hyperphosphorylated tau as well as neurodegeneration (Jack et al., 2018). In limbic-dominant AD, a progressive decline in episodic memory function is the cardinal cognitive symptom (Vogel et al., 2021). Episodic memory is defined as the memory of events that were experienced in a particular time and location (Tulving, 1983). AD has been associated with impairment in encoding (Golby et al., 2005; Sperling et al., 2003), consolidation (Borlikova et al., 2013; Freir et al., 2011), and retrieval (Murphy et al., 2008) of experienced episodes.

Disease progression along the AD continuum is assumed to begin with increasing levels of Aβ. Later, elevated biomarkers of tau and neurodegeneration can be observed (Jack et al., 2018). Notably, patients may not experience cognitive symptoms as late as 15 to 20 years after exhibiting first detectible Aβ pathology (Jansen et al., 2015). This preclinical stage of AD is followed by a prodromal stage in which patients have mild cognitive impairment (MCI). With increasing pathology, a large proportion of patients fulfills diagnostic criteria for dementia (Jack et al., 2018). Previous research suggests that AD-related cognitive impairment is primarily a consequence of neurodegeneration, particularly in the medial temporal lobe (MTL), which, in turn, is caused by proteinopathy (Jack et al., 2009; Mormino et al., 2009). However, recent studies reported earliest cognitive impairment to occur independent of neurodegeneration (Bejanin et al., 2017; Berron et al., 2021). Hence, further research is needed to test if the association of proteinopathy and cognitive decline is fully mediated by neurodegeneration or if, especially in earlier AD stages, there are alternative mechanisms causing cognitive impairment.

Domain-specific episodic memory in AD

Previous studies using anatomical and functional imaging methods identified two cortico-hippocampal memory and information processing networks: a posterior-medial (PM) network, including posterior cingulate cortex (PCC), precuneus (Prec), angular gyrus, anterior thalamus, medial prefrontal cortex, and parahippocampal cortex (PhC), and an anterior-lateral (AL) network, comprising amygdala, anterior ventral temporal cortex, lateral orbitofrontal cortex (lOFC), and perirhinal cortex (PrC; Inhoff & Ranganath, 2017; Ritchey et al., 2015). The two cortical networks are integrated in the hippocampus mainly via entorhinal pathways (Agster & Burwell, 2013; Libby et al., 2014). In terms of their functional preferences, the PM network processes spatial and contextual information while the AL network primarily handles information on content and items (Inhoff & Ranganath, 2017; Ritchey et al., 2015).

Since the introduction of Aβ and later tau positron emission tomography (PET) radiotracers, the spatial distribution of proteinopathy along the AD continuum has been increasingly understood. For tau, the results obtained in PET studies largely correspond to earlier histopathological autopsy studies, strengthening the assumption of stereotypical tau spreading (Schöll et al., 2016; Schwarz et al., 2016). Tau accumulation is assumed to follow a spatiotemporal pattern that is commonly described using the Braak staging framework. Here, six stages of tau pathology are defined (Braak stages I-VI; Braak & Braak, 1991): Initially, tau depositions can be found in the transentorhinal region, which overlaps with Brodmann area (BA) 35 and parts of the entorhinal cortex. This stage is followed by further depositions in the medial and basal temporal lobes before other isocortical regions are affected. In earlier stages of AD, sites of tau aggregation overlap with regions of the AT system. With progression of the disease, tau starts being detectible in regions of the PM system, too (Berron et al., 2021; Ossenkoppele et al., 2018; Pascoal et al., 2020). Meanwhile, Aβ is found

in isocortical regions of the PM system in earliest stages of AD before diffusely spreading throughout the cortex (Palmqvist et al., 2017; Villeneuve et al., 2015). The different spatiotemporal trajectories of tau and Aβ accumulations may reflect in a distinctly progressing object- and scene-based episodic memory impairments along the AD continuum. In fact, Maass et al. (2019) reported negative relationships of AT tau with object-based mnemonic discrimination and PM Aβ with scene-based mnemonic discrimination in a sample of healthy controls and older adults who were either cognitively unimpaired (CU), had MCI, or AD dementia. However, other studies support the notion of domain-specific memory loss being primarily driven by tau rather than Aβ, suggesting that PM-based function decreases only in the presence of local tau (Berron et al., 2019; Stark & Stark, 2017). Given the inconclusive results and small number of published studies, further research is needed to identify the causal mechanisms underlying domain-specific episodic memory loss and its relationship with AD pathology.

Subregional distinctions within the MTL

The MTL is essential for episodic memory (Eichenbaum et al., 2007) and its vulnerability to AD-related neurodegeneration is assumed to explain the large proportion of AD patients experiencing amnestic symptoms (Jagust, 2018). However, this vulnerability differs considerably among subregions of the MTL. Tau is first found in the transentorhinal region and, inside the hippocampus, at the border of cornu ammonis (CA) 1 and subiculum (Sub). Later, tau accumulates in the whole entorhinal cortex (ErC) and CA1 as well as other hippocampal subfields (i.e., CA2; dentate gyrus, DG; and CA3) and parahippocampal regions of the MTL (Lace et al., 2009). Additionally, MTL subregions are differently involved in the PM and AT systems. Specifically, the PrC and AL ErC are associated with the AL network while the PhC and PM ErC are embedded in the PM network (Inhoff & Ranganath, 2017).

Moreover, hippocampal subfields have been linked to different processes and operations of episodic memory. DG has been found to contribute to pattern separation (Neunuebel & Knierim, 2014), the process of reducing interference by assigning distinct memory traces to similar information (Yassa & Stark, 2011). Meanwhile, retrieving information from incomplete cues is facilitated by pattern completion which has been associated with activity in CA3 (Neunuebel & Knierim, 2014). While previous studies report AD-related atrophy in different hippocampal subfields (e.g., de Flores et al., 2015; Müller-Ehrenberg et al., 2018; Wisse et al., 2014), the relationships of hippocampal subfield atrophy, proteinopathy, and cognition, especially in early AD stages, has not been resolved yet. Importantly, neuroimaging studies of MTL subregions face the problem that most automated segmentation tools do not consider interindividual anatomical differences. In fact, characteristics of certain anatomical hallmarks can have a substantial influence on how MTL subregions are defined on an individual level (Ding & Van Hoesen, 2010). Especially in larger samples, manual segmentation is often not feasible, leading to deficient anatomical precision.

Possible facets of AD-related alterations in episodic memory

Paradigms testing recognition memory commonly use new (i.e., not previously studied) and old (i.e., previously studied) stimuli for each of which participants are asked to judge if it was presented before. While most studies following this schema focus on participants' ability to tell apart studied and unstudied stimuli (mnemonic discrimination), differences in response bias are often neglected. Response bias refers to someone's tendency to respond "new" or "old" when actually being uncertain (Snodgrass & Corwin, 1988). In such instances, individuals with a liberal response bias tend towards responding "new" whereas those with a conservative response bias rather respond "old". When solely focusing on mnemonic discrimination, one neglects that a certain discrimination performance can be

the result of a wide range of response tendencies and/or strategies. For instance, high hit rates (HRs; i.e., correctly identifying a studied stimulus as old) accompanied by high false alarm rates (FARs; i.e., falsely identifying an unstudied stimulus as old) reflect a similar level of mnemonic discrimination to low HRs accompanied by low FARs. Yet, the response biases underlying these performance outcomes are fundamentally different – high HRs with high FARs are the results of a liberal response bias and low HRs with low FARs indicate a conservative response bias.

Budson et al. (2006) demonstrated why considering response bias adds a valuable behavioral dimension when studying recognition memory in (pathological) aging. In their study, AD patients exhibited a more liberal response bias in a verbal memory task compared to healthy older adults. This effect remained when matching the two groups for discrimination performance. Further previous studies reported similar findings of AD patients exhibiting a more liberal response bias (Deason et al., 2017; Russo et al., 2017). However, a recent study did not find evidence of AD-related changes in response bias (van den Berg et al., 2020). Generally, AD-related changes in response bias are not well understood as previous evidence is inconclusive. Most earlier studies also lack AD biomarker data and, hence, cannot answer how Aβ and tau burden are related to response bias.

The present study

With the present study, I pursue three objectives. First, my study tests if memory decline along the AD continuum differs between object- and scene-based episodic memory. Second, I aim to identify where on the AD continuum earliest regional atrophy in the PM and AL networks can be observed. Third, I investigate if early Aβ and tau burden as well as regional PM and AL atrophy are related to domain-specific mnemonic discrimination and

response bias. Fourth, I test if the relationship of Aβ and tau burden with domain-specific mnemonic discrimination and response bias is mediated by regional PM and AL atrophy.

Older adults who were CU and Aβ-negative (CU Aβ-), CU and Aβ-positive (CU Aβ+), or had AD-related MCI (MCI Aβ+) were recruited from the Swedish BioFINDER-2 (BF-2) cohort. Participants underwent high-resolution structural MRI (sMRI) at 7 Tesla (T) field strength, 3 T sMRI, as well as [^{18}F]Flutemetamol and [^{18}F]RO948 PET. Indicators of object- and scene-based mnemonic discrimination and response bias were obtained using a mnemonic discrimination task.

Methods

Participants

Participants were allocated a diagnostic group based on their cognitive and Aβ statuses. Participants were either cognitively unimpaired (CU) or exhibited mild cognitive impairment (MCI). Inclusion criteria for the CU group were (a) being aged ≥ 50 years old, (b) a Mini Mental State Examination (MMSE; Folstein et al., 1975) score ≥ 26, (c) not fulfilling the criteria for MCI or dementia according to DSM-5 (American Psychiatric Association, 2013), (d) exhibiting no cognitive symptoms as assessed by a physician, and (e) being fluent in Swedish. Inclusion criteria for the MCI group were (a) being aged ≥ 50 years old, (b) having been referred to a memory clinic due to cognitive symptoms, (c) an MMSE score ≥ 24, (d) not fulfilling the DSM-5 criteria for dementia, and (e) a performance lower than –1.5 SD in at least one cognitive domain assessed through a neuropsychological test battery with respect to age and education stratified norms. The neuropsychological test battery covered the following cognitive domains: attention/executive function (Trail Making Test A and B; Reitan, 1955; and Symbol Digit Modalities Test; Smith, 1982), memory (10-word immediate and delayed recall from the Alzheimer's Disease Assessment Scale; Mohs, 1996), verbal

ability (animal fluency and the 15-word short version of the Boston Naming Test, Kaplan et al., 2001), and visuospatial function (incomplete letters and cube analysis from the Visual Object and Space Perception battery; Warrington & James, 1991). Aβ status was determined using CSF $A\beta_{42}/A\beta_{40}$ ratio. The cutoff of 0.63 determining Aβ positivity was obtained using Gaussian mixture modeling. In the present study, CU Aβ-, CU Aβ+, and MCI Aβ+ groups were distinguished.

Out of $N = 144$ recruited participants, $n = 121$ (60 CU Aβ-, 41 CU Aβ+, 20 MCI Aβ+) were included in the final sample. Exclusions were due to missing structural MRI data ($n = 4$), insufficient quality of MTL segmentations ($n = 3$), missing data from the mnemonic discrimination task ($n = 10$), mean mnemonic discrimination performance equal to or lower than chance (details in ***Mnemonic discrimination task***) and/or irregularities during the mnemonic discrimination task indicating invalid performance ($n = 6$). Aβ-PET was missing for one CU Aβ- participant. Tau-PET was available for the whole sample. Participants gave written informed consent to participate and were informed that they could withdraw from the study at any time. The study was approved by the ethical review board in Lund, Sweden.

Materials and measures

Imaging

sMRI. To obtain measures of subregional PM and AL cortical thickness, participants underwent 3T sMRI in a Siemens 3 T MAGNETOM Prisma MR system (Siemens Medical Solutions). Whole-brain T1-weighted images with 1mm isotropic voxels were obtained using a magnetization-prepared rapid gradient echo (MPRAGE) sequence. Whole-brain T2-weighted images with 0.4 x 0.4 x 2.0 mm voxels were collected using Turbo Spin Echo (TSE) imaging. Detailed multi-atlas segmentation of the MTL was performed using the Automated Segmentation of Hippocampal Subfields algorithm (ASHS; Yushkevich et al.,

2015). ASHS is a publicly available, open-source multi-atlas joint label fusion (JFL) algorithm which generates MTL segmentation masks from an atlas of manually segmented images (https://sites.google.com/view/ashs-dox/cloud-ashs/cloud-ashs-for-t2-mri; Yushkevich et al., 2015). Importantly, one of the advantages of using ASHS is that it considers neuroanatomical features (e.g., depth of the collateral sulcus) for high precision of MTL segmentations. Outside the MTL, FreeSurfer (v6.0; http://surfer.nmr.mgh.harvard.edu) was used to obtain average cortical thickness for PM (inferior parietal cortex, IPC; isthmus cingulate, IsthCing; lateral occipital cortex, LOC; medial orbitofrontal cortex, mOFC; PCC; Prec) and AL ROIs (inferior temporal cortex, ITC; lOFC; temporal pole, TP).

Hippocampal subfield volumetry was obtained using a 7 T Philips Achieva AS MR system (Philips Healthcare). High-resolution (0.4 x 0.4 x 1.00 mm voxel size) T2-weighted TSE imaging captured a slab covering the whole coronal plane and the entire length of the hippocampus on the posterior-anterior axis. Additionally, T1-weighted whole-brain MPRAGE images with 0.7mm^3 isotropic voxels were obtained. ASHS was used to derive ROI-based gray matter volumes (GMVs) for CA1, CA2/3, DG, Sub, and hippocampal tail (HT). GMVs were adjusted for intracranial volume (ICV; $\mathrm{GMV}_{\mathrm{adj.}} = \frac{\mathrm{GMV} \cdot 10000}{\mathrm{ICV}}$). In n = 8 participants (1 CU Aβ-, 3 CU Aβ+, 4 MCI Aβ+), image quality at 7 T was insufficient for hippocampal subfield segmentation. In these cases, hippocampal subfield GMVs were derived from 3 T sMRI. In the whole sample, the average time interval between 3 T and 7 T sMRI was –117 days (SD = 201.82; min = –489; max = 347)

All subregional masks were visually assessed. Hippocampal subregional masks were edited if required. ASHS includes a machine learning algorithm which is designed to correct systematic errors of JFL results at voxel level (Wang et al., 2011). After visual inspection of JFL results before and after correction, it was decided to use corrected masks for 3 T sMRI images and uncorrected masks for 7T sMRI images.

PET. PET data was acquired on a digital GE Discovery MI PET/CT system (General Electric Medical Systems). Aβ PET was performed 90–100 min. after the injection of ~185 MBq [^{18}F]Flutemetamol. Standardized uptake value ratio (SUVr) images were calculated for a region of interest (ROI) exhibiting earliest Aβ in AD (for details, see Palmqvist et al., 2017) using the entire cerebellum for reference (Thurfjell et al., 2014). For tau PET, dynamic LIST-mode acquisition was performed 70–90 min. after the injection of 365±20 MBq of [^{18}F]RO948. SUVr images were calculated for an ROI corresponding to the tau accumulation sites of Braak stages I and II (Braak & Braak, 1991) with the inferior cerebellum as the reference region (Baker et al., 2017). PET images were registered and normalized to a template calculated from 3 T T1-weighted MPRAGE images. Approval for tau PET was given by the Swedish Medical Products Agency.

Mnemonic discrimination task

Participants performed a mnemonic discrimination task during a functional MRI scan which was acquired during the same session as the 7 T sMRI scan. The mnemonic discrimination task has been used previously in similar settings and samples (e.g., Adams et al., 2021; Berron et al., 2018; Maass et al., 2019). Participants were presented sequences of four stimuli. A sequence could contain stimuli of only objects or scenes. While the first two stimuli were always new, the subsequent two stimuli were either an exact repetition or a slightly modified version (lure) of one of the first two stimuli in the sequence. Participants were asked to indicate for each stimulus whether it was new (i.e., the stimulus had not been presented before) or old (i.e., the stimulus had been presented before). Participants were instructed that similar, but not identical, stimuli should be considered new. Before scanning, participants performed a short training outside the scanner to familiarise with the task. During the fMRI scan, participants completed a total of 128 sequences (i.e., 256 trials). As the

number of trials was balanced across domains and stimulus pairings, 32 first-repeat pairs and 32 first-lure pairs were presented per domain. A detailed description of the mnemonic discrimination task can be found in a previous publication by Berron et al. (2018).

Following the recommendations by Snodgrass & Corwin (1988), *Pr* and *Br* were chosen as indices of discrimination and response bias, respectively. To obtain the two behavioural outcomes, HRs and FARs were calculated for each domain as follows:

$$\mathrm{HR}_{\mathrm{domain}} = \frac{\mathrm{hits}_{\mathrm{domain}}+0.5}{\mathrm{repetitions}_{\mathrm{domain}}+1}; \mathrm{FAR}_{\mathrm{domain}} = \frac{\mathrm{false\ alarms}_{\mathrm{domain}}+0.5}{\mathrm{lures}_{\mathrm{domain}}+1}$$

Pr is a measure of discrimination that, under the assumption that FARs and HRs are inversely related, corrects HRs for the influence of lucky guesses made in uncertainty and is calculated using:

$$Pr_{\mathrm{domain}} = \mathrm{HR}_{\mathrm{domain}} - \mathrm{FAR}_{\mathrm{domain}}$$

Pr can range between –1 and 1 with higher values indicating better discrimination. As $Pr = 0$ can be achieved by random responding, only cases of $Pr > 0$ were included. This criterion was applied to mean *Pr*s across domains as $Pr > 0$ in one domain was assumed to reflect that the task was generally understood by the participants.

The bias index *Br* can be expressed as follows:

$$Br_{\mathrm{domain}} = \frac{\mathrm{FAR}_{\mathrm{domain}}}{1 - (\mathrm{HR}_{\mathrm{domain}} - \mathrm{FAR}_{\mathrm{domain}})}$$

Br can range between 0 and 1, with 0.5 indicating a balanced response bias. $Br < 0.5$ reflects a conservative bias while $Br > 0.5$ corresponds to a liberal bias.

Statistical analyses

All statistical analyses were implemented in R (v.4.0.5; www.r-project.org). The threshold for statistical significance was two-sided and set at $p < .05$ at all times. Correction for multiple comparisons using False-Discovery Rate detection was applied where required.

To test for interaction effects of diagnostic group and domain on *Pr*s and *Br*s, two two-way mixed analyses of covariance (ANCOVAs) were conducted. The models included diagnostic group, domain, and their interaction as independent variables as well as age, sex, and years of education as control variables. To test for differences between diagnostic groups in regional atrophy measures, one-way independent ANCOVAs were calculated for each sMRI outcome (i.e., hippocampal $GMVs_{adj}$ and extrahippocampal cortical thicknesses). Age was included as a covariate. For all ANCOVA models, dependent variables were log-tranformed if heterogeneous variances were identified by Levene tests using the leveneTest function in the car package (v.3.0-10; Fox & Weisberg, 2019). Covariate-adjusted outcome means were obtained using the effects function in the stats package (v.3.6.2; R Core Team, 2021). Tukey *post-hoc* tests, implemented in the glht function from the multcomp package (v.1.4-16; Hothorn et al., 2008), were used to follow up significant main effects by calculating pairwise contrasts. Effect sizes partial η^2 and Cohen's *d* were obtained using the etaSquared function from the lsr package (v.0.5; Navarro, 2015) and the mes function compute.es package (v.0.2-5; Del Re, 2013), respectively. As age was included as a covariate and one-way analysis of variance revealed that groups differed in age ($F(2, 118) = 8.34$, $p < .001$, partial $\eta^2 = .12$), an age-balanced subsample was used to calculate the ANCOVAs (n = 108, 12 CU Aβ- and 1 CU Aβ+ excluded).

To investigate the relationship of Aβ and tau SUVrs as well as regional atrophy measures with task outcomes, multiple linear regression models were calculated. Each model predicted a task outcome by a PET or sMRI measure and was calculated for the whole sample and for each diagnostic group separately. All multiple linear regression models included age, sex, and years of education as a covariate. If a model showed a significant effect of an sMRI measure on a task outcome, it was tested if this relationship was part of a mediation effect of atrophy on the association of proteinopathy and cognition. For each identified pair of sMRI

measure and task outcome, one mediation model using Aβ SUVr and another mediation model using tau SUVr as the independent variable were calculated. Mediation analyses were run using the mediate function in the mediation package (v.4.5.0; Tingley et al., 2014) with 95% confidence intervals (CIs) being generated through quasi-Bayesian Monte Carlo simulations. In all linear models, outliers with high leverage were excluded if their Cook's distance exceeded the cutoff of 4/*N* (Altman & Krzywinski, 2016).

Results

Sample characteristics

An overview of whole sample and the diagnostic groups is provided in Table 1. Characteristics of the ANCOVA subsample can be found in the appendix (Table A1).

Interaction effects of domain and diagnostic group on task outcomes

For *Pr*s, ANCOVAs showed significant main effects of age ($F(1, 197) = 80.09$, $p < .001$, partial $\eta^2 = .23$), years of education ($F(1, 197) = 6.23$, $p = .013$, $r = .17$, partial $\eta^2 = .03$), diagnostic group ($F(2, 197) = 6.29$, $p = .002$, partial $\eta^2 = .07$), and domain ($F(1, 197) = 38.72$, $p < .001$, partial $\eta^2 = .11$). Tukey *post-hoc* tests revealed lower *Pr*s in the scene condition ($M_{adj.} = 0.21$, 95% CI [0.19; 0.23]) compared to *Pr*s in the object condition ($M_{adj.} = 0.32$, 95% CI [0.29; 0.34]; $t = –5.03$, $p < .001$, $d = 0.61$). *Pr*s in the MCI Aβ+ group ($M_{adj.} = 0.21$, 95% CI [0.17; 0.25]) were significantly lower than in the CU Aβ- ($M_{adj.} = 0.26$, 95% CI [0.24; 0.29], $t = –3.04$, $p = .007$, $d = –0.25$) and CU Aβ+ ($M_{adj.} = 0.29$, 95% CI [0.27; 0.32], $t =– 3.76$, $p < .001$, $d = –0.37$) groups. The interaction effect of diagnostic group and domain was not significant ($F(2, 197) = 2.26$, $p = .107$, partial $\eta^2 = .02$). In the adjusted means, a trend towards lower *Pr*s in the object condition could be observed in the MCI Aβ+ group ($M_{adj.} = 0.22$, 95% CI [0.17; 0.28]) compared to the CU Aβ- ($M_{adj.} = 0.33$, 95% CI

Table 1

Sample characteristics

	CU Aβ-	CU Aβ+	MCI Aβ+	Whole Sample
n	60	41	20	121
Females (%)	29 (48.33%)	21 (51.22%)	11 (55.00%)	61 (50.41%)
Age (SD)	65.52 (10.35)	70.98 (8.00)	73.70 (4.81)	68.72 (9.42)
Years of education (SD)	12.79 (3.12)	11.95 (2.99)	11.82 (4.22)	12.35 (3.28)
Pr (objects) (SD)	0.38 (0.20)	0.37 (0.20)	0.19 (0.11)	0.35 (0.20)
Pr (scenes) (SD)	0.26 (0.16)	0.23 (0.13)	0.17 (0.11)	0.23 (0.15)
Br (objects) (SD)	0.77 (0.22)	0.74 (0.21)	0.74 (0.26)	0.75 (0.22)
Br (scenes) (SD)	0.74 (0.21)	0.74 (0.17)	0.73 (0.21)	0.74 (0.19)
Early Aβ ROI SUVr (SD)	0.64 (0.03)	0.91 (0.18)	1.01 (0.20)	0.80 (0.20)
Braak I/II tau SUVr (SD)	1.25 (0.18)	1.54 (0.40)	1.86 (0.38)	1.45 (0.38)
MMSE (SD)	28.97 (1.12)	28.66 (1.37)	27.15 (2.03)	28.56 (1.52)
ADAS delayed word recall (SD)	2.62 (1.81)	3.32 (1.85)	6.65 (2.60)	3.52 (2.43)
Symbol Digit Modalities Test (SD)	43.53 (11.73)	38.62 (10.57)	28.00 (8.52)	39.40 (12.11)
Animal fluency (SD)	24.50 (6.43)	22.37 (6.15)	14.10 (5.58)	22.06 (7.17)

Note. ADAS = Alzheimer's Disease Assessment Scale. Aβ = amyloid-β. CU = cognitively unimpaired. MCI = mild cognitive impairment. ROI = region of interest. SD = standard deviation. SUVr = standardized uptake value ratio.

[0.29; 0.36]) and CU Aβ+ ($M_{adj.}$ = 0.35, 95% CI [0.31; 0.39]) groups. *Pr*s in the scene condition were relatively stable across groups (CU Aβ-: $M_{adj.}$ = 0.20, 95% CI [0.16; 0.23], CU Aβ+: $M_{adj.}$ = 0.24, 95% CI [0.20; 0.28]; MCI Aβ+: $M_{adj.}$ = 0.19, 95% CI [0.14; 0.25]).

For *Br*s, age (F (1, 195) = 5.33, p = .022, partial η^2 = .01) and years of education (F (1, 195) = 11.63, p = .001, partial η^2 = .06) exhibited significant main effects. There were no significant main effects of sex (F (1, 195) = 0.66, p = .418, partial η^2 = .00), diagnostic group (F (2, 195) = 0.34, p = .710, partial η^2 = .00), or domain (F (1, 195) = 0.00, p = .999, partial η^2 = .00) as well as no significant interaction effect of diagnostic group and domain (F (2, 195) = 0.00, p = .999, partial η^2 = .00). Figure 1 displays the covariate-adjusted means of *Pr*s and *Br*s and their 95% CIs in each diagnostic group.

Diagnostic group differences in regional atrophy measures

ANCOVAs showed a significant effect of diagnostic group on CA2/3 GMV_{adj} ($F(2, 101) = 6.26$, $p_{fdr} = .014$, partial $\eta^2 = .09$). Tukey *post-hoc* tests were significant for the contrasts of MCI Aβ + versus CU Aβ- ($t = –2.90$, p = .012, d = –0.40) and MCI Aβ+ versus CU Aβ+ ($t = –3.49$, $p = .002$, $d = –0.47$). There was no significant difference between the CU Aβ+ and CU Aβ- groups in CA2/3 $GMV_{adj.}$ ($t = 0.81$, $p = .693$, $d = 0.11$). In CA1 ($F(2, 99) = 3.79$, $p_{fdr} = .057$, partial $\eta^2 = .09$), DG ($F(2, 98) = 4.10$, $p_{fdr} = .057$, partial $\eta^2 = .09$), Sub ($F(2, 102) = 3.10$, $p_{fdr} = .059$, partial $\eta^2 = .07$), and HT ($F(2, 99) = 2.86$, $p_{fdr} = .068$, partial $\eta^2 = .07$), effects of diagnostic group on GMV_{adj} were significant before but not after FDR correction. In all of these outcomes, there was a trend towards lower $GMVs_{adj}$ in MCI Aβ+ group versus the CU Aβ+ group. Surprisingly, all hippocampal subfield $GMVs_{adj}$ except HT $GMVs_{adj}$ tended towards being larger in the CU Aβ+ group than in the CU Aβ- group. This

Figure 1

Mean values of mnemonic discrimination task outcomes across diagnostic groups

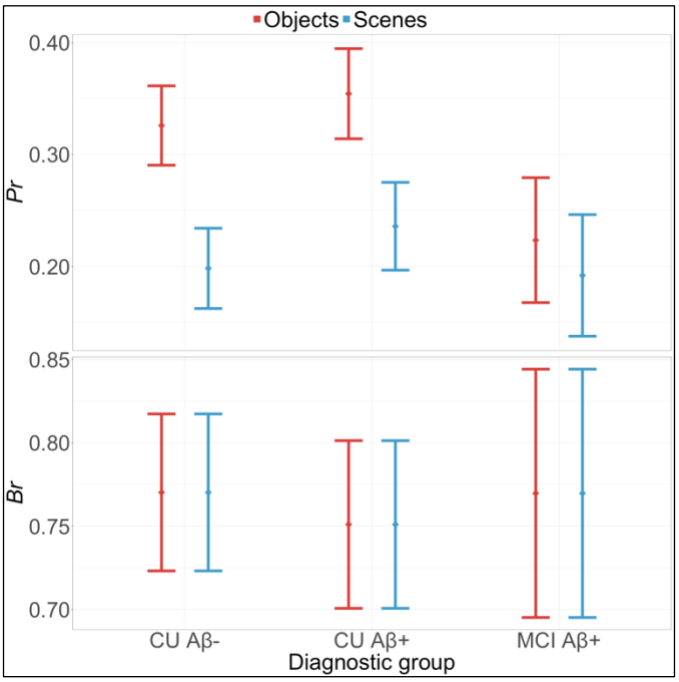

Note. Mean values are adjusted for age, sex, and years of education. The error bars display 95% confidence intervals. Aβ = amyloid-β. CU = cognitively unimpaired. MCI = mild cognitive impairment

trend could be observed in raw and adjusted means but did not reach statistical significance before or after FDR correction. There were no significant effects of diagnostic group on median cortical thickness in ErC ($F(2, 100) = 1.08$, $p_{fdr} = .415$, partial $\eta^2 = .02$), BA35 ($F(2, 101) = 3.66$, $p_{fdr} = .235$, partial $\eta^2 = .04$), BA36 ($F(2, 99) = 1.97$, $p_{fdr} = .235$, partial $\eta^2 = .03$), and PhC ($F(2, 104) = 0.35$, $p_{fdr} = .830$, partial $\eta^2 = .01$) ROIs, or on average cortical thickness of IPC ($F(2, 103) = 2.11$, $p_{fdr} = .235$, partial $\eta^2 = .04$), IsthCing ($F(2, 100) = 1.77$, $p_{fdr} = .254$, partial $\eta^2 = .03$), LOC ($F(2, 99) = 0.09$, $p_{fdr} = .963$, partial $\eta^2 = .00$), mOFC ($F(2, 98) = 3.37$, $p_{fdr} = .235$, partial $\eta^2 = .05$), PCC ($F(2, 100) = 2.13$, $p_{fdr} = .235$, partial $\eta^2 = .05$), Prec ($F(2, 101) = 1.08$, $p_{fdr} = .415$, partial $\eta^2 = .01$), ITC ($F(2, 101) = 3.94$, $p_{fdr} = .235$, partial $\eta^2 = .05$),

Figure 2

Mean values sMRI outcomes across diagnostic groups

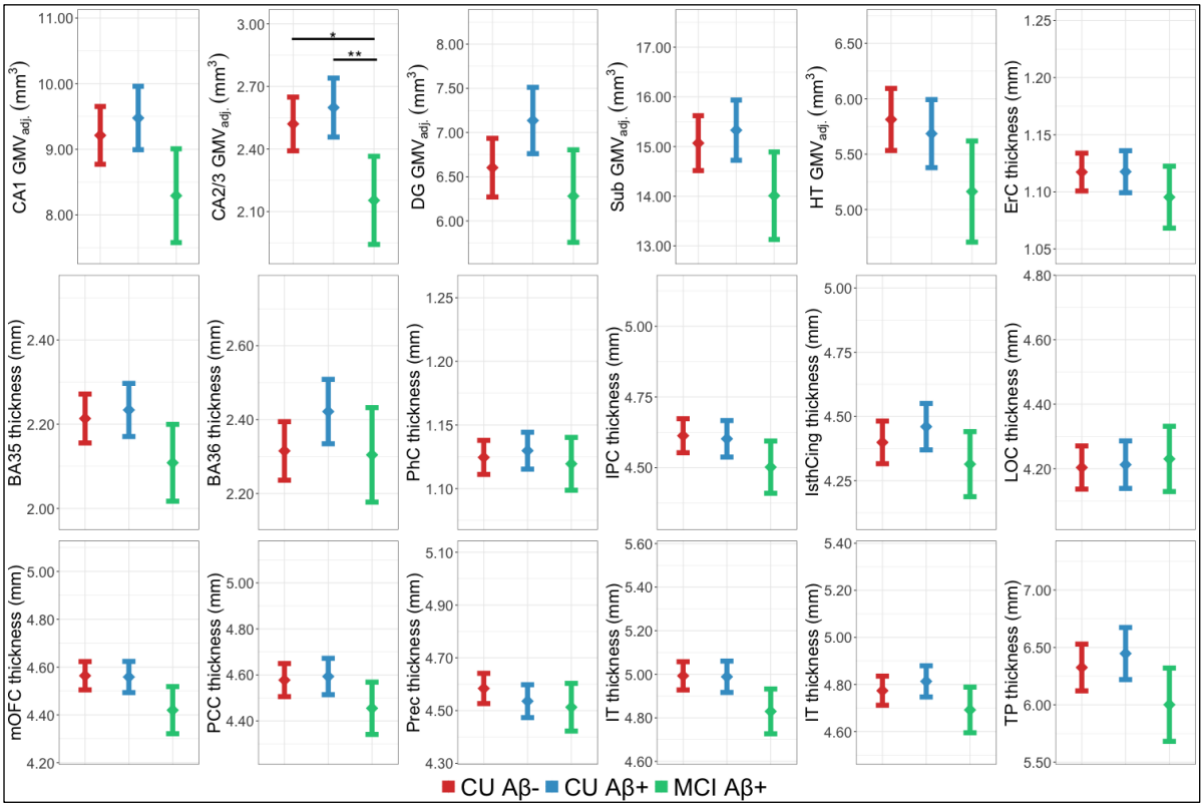

Note. Mean values in are adjusted for age. The error bars display 95% confidence intervals. $^{**}p_{fdr} < .01$. $^{*}p_{fdr} < .05$. Aβ = amyloid-β. BA = Brodmann area. CA = cornu ammonis. CU = cognitively unimpaired. DG = dentate gyrus. ErC = entorhinal cortex. GMV = gray matter volume. HT = hippocampal tail. IPC = inferior parietal cortex. IsthCing = isthmus cingulate. ITC = inferior temporal cortex. LOC = lateral occipital cortex. lOFC = lateral orbitorfrontal cortex. MCI = mild cognitive impairment. mOFC = medial orbitorfrontal cortex. Sub = subiculum. TP = temporal pole. PCC = posterior cingulate cortex. PhC = parahippocampal cortex. Prec = Precuneus

Table 2

Differences in sMRI outcomes between the diagnostic groups

	n	**Raw means (SD)**			**Adjusted means [95% CI]**			**Coefficients (*F* (df))**			**Tukey *post-hoc* tests (*t*)**		
		CU Aβ-	CU Aβ+	MCI Aβ+	CU Aβ-	CU Aβ+	MCI Aβ+	Intercept	Age	Diagnostic group	CU Aβ+ *vs.* CU Aβ-	MCI Aβ+ *vs.* CU Aβ-	MCI Aβ+ *vs.* CU Aβ+
CA1 $GMV_{adj.}$ (mm^3)	103	9.35 (1.61)	9.42 (1.54)	8.03 (1.67)	9.21 [8.77; 9.65]	9.48 [8.99; 9.96]	8.29 [7.58; 9.01]	113.70 (1, 99)	14.49 (1, 99) **	3.79 (2, 99)			
CA2/3 $GMV_{adj.}$ (mm^3)	105	2.54 (0.47)	2.59 (0.45)	2.11 (0.44)	2.52 [2.39; 2.65]	2.60 [2.46; 2.74]	2.15 [1.94; 2.36]	78.67 (1, 101)	6.37 (1, 101) *	6.26 (2, 100)*	0.81	–2.90	–3.49**
DG $GMV_{adj.}$ (mm^3)	102	6.66 (0.99)	7.12 (1.23)	6.19 (1.36)	6.60 [6.27; 6.93]	7.14 [6.76; 7.51]	6.28 [5.76; 6.8]	70.01 (1, 98)	4.32 (1, 98) *	4.10 (2, 98)	–	–	–
Sub $GMV_{adj.}$ (mm^3)	106	15.26 (1.82)	15.26 (2.21)	13.67 (2.34)	15.07 [14.52; 15.62]	15.33 [14.72; 15.94]	14.01 [13.13; 14.89]	176.24 (1, 102)	18.94 (1, 102) ***	3.10 (2, 102)	–	–	–
HT $GMV_{adj.}$ (mm^3)	103	5.88 (0.87)	5.67 (1.02)	5.03 (1.18)	5.81 [5.53; 6.09]	5.69 [5.38; 5.99]	5.16 [4.71; 5.62]	87.10 (1, 99)	6.79 (1, 99) *	2.86 (2, 99)	–	–	–
ErC median thickness (mm)	104	1.12 (0.05)	1.12 (0.06)	1.09 (0.07)	1.12 [1.1; 1.13]	1.12 [1.1; 1.14]	1.10 [1.07; 1.12]	510.23 (1, 100)	0.82 (1, 100)	1.08 (2, 100)	–	–	–
BA35 median thickness (mm)	105	2.23 (0.23)	2.23 (0.18)	2.08 (0.20)	2.21 [2.16; 2.27]	2.23 [2.17; 2.3]	2.11 [2.02; 2.2]	262.65 (1, 101)	14.81 (1, 101) ***	2.66 (2, 101)	–	–	–
BA36 median thickness (mm)	103	2.33 (0.26)	2.41 (0.28)	2.28 (0.32)	2.32 [2.24; 2.39]	2.42 [2.33; 2.51]	2.30 [2.18; 2.43]	143.10 (1, 99)	5.99 (1, 99) *	1.97 (2, 99)	–	–	–
PhC median thickness (mm)	108	1.13 (0.05)	1.13 (0.04)	1.11 (0.07)	1.12 [1.11; 1.14]	1.13 [1.12; 1.14]	1.12 [1.1; 1.14]	1033.67 (1, 104)	21.82 (1, 104) ***	0.35 (2, 104)	–	–	–
IPC average thickness (mm)	107	4.64 (0.25)	4.59 (0.24)	4.46 (0.21)	4.61 [4.55; 4.67]	4.60 [4.54; 4.67]	4.50 [4.41; 4.59]	976.46 (1, 103)	36.80 (1, 103) ***	2.11 (2, 103)	–	–	–
IsthCing average thickness (mm)	104	4.41 (0.29)	4.46 (0.30)	4.29 (0.24)	4.40 [4.32; 4.48]	4.46 [4.37; 4.55]	4.31 [4.19; 4.44]	383.10 (1, 100)	5.79 (1, 100) *	1.77 (2, 100)	–	–	–
LOC average thickness (mm)	103	4.23 (0.24)	4.20 (0.24)	4.20 (0.24)	4.20 [4.14; 4.27]	4.21 [4.14; 4.29]	4.23 [4.13; 4.33]	590.14 (1, 99)	13.51 (1, 99) **	0.09 (2, 99)	–	–	–
mOFC average thickness (mm)	102	4.57 (0.17)	4.56 (0.20)	4.41 (0.28)	4.56 [4.5; 4.62]	4.56 [4.49; 4.62]	4.42 [4.32; 4.52]	686.44 (1, 98)	3.17 (1, 98)	3.37 (2, 98)	–	–	–
PCC average thickness (mm)	104	4.58 (0.23)	4.59 (0.26)	4.45 (0.25)	4.58 [4.51; 4.65]	4.59 [4.51; 4.67]	4.45 [4.34; 4.57]	455.74 (1, 100)	0.48 (1, 100)	2.13 (2, 100)	–	–	–
Prec average thickness (mm)	105	4.60 (0.20)	4.53 (0.21)	4.48 (0.24)	4.58 [4.53; 4.64]	4.54 [4.47; 4.6]	4.51 [4.42; 4.6]	881.92 (1, 101)	14.88 (1, 101)**	1.08 (2, 101)	–	–	–

Table 2 ***(continued)***

Differences in task and sMRI outcomes between the diagnostic groups

	n	**Raw means (SD)**			**Adjusted means [95% CI]**			**Coefficients (*F* (df))**			**Tukey *post-hoc* tests (*t*)**		
		CU Aβ-	CU Aβ+	MCI Aβ+	CU Aβ-	CU Aβ+	MCI Aβ+	Intercept	Age	Diagnostic group	CU Aβ+ *vs.* CU Aβ-	MCI Aβ+ *vs.* CU Aβ-	MCI Aβ+ *vs.* CU Aβ+
ITC average thickness (mm)	105	5.02 (0.23)	4.98 (0.27)	4.79 (0.22)	4.99 [4.93; 5.06]	4.99 [4.92; 5.06]	4.83 [4.73; 4.93]	879.08 (1, 101) ***	21.66 (1, 101) ***	3.94 (2, 101)	–	–	–
lOFC average thickness (mm)	106	4.78 (0.20)	4.81 (0.19)	4.68 (0.27)	4.77 [4.71; 4.84]	4.81 [4.75; 4.88]	4.69 [4.6; 4.79]	725.07 (1, 102)	2.86 (1, 102)	2.12 (2, 102)	–	–	–
TP average thickness (mm)	103	6.40 (0.64)	6.41 (0.82)	5.90 (0.82)	6.33 [6.12; 6.53]	6.45 [6.22; 6.67]	6.00 [5.68; 6.32]	193.57 (1, 99)	15.82 (1, 99) ***	2.59 (2, 99)	–	–	–

Note. All reported *p*-values were corrected for false discovery rate. ***$p_{fdr} < .001$. ** $p_{fdr} < .01$. * $p_{fdr} < .05$. Aβ = amyloid-β. BA = Brodmann area. CA = cornu ammonis. CU = cognitively unimpaired. DG = dentate gyrus. DV = dependent variable. ErC = entorhinal cortex. GMV = gray matter volume. HT = hippocampal tail. IPC = inferior parietal cortex. IsthCing = isthmus cingulate. ITC = inferior temporal cortex. LOC = lateral occipital cortex. lOFC = lateral orbitorfrontal cortex. MCI = mild cognitive impairment. mOFC = medial orbitorfrontal cortex. Sub = subiculum. TP = temporal pole. PCC = posterior cingulate cortex. PhC = parahippocampal cortex. Prec = Precuneus.

lOFC ($F(2, 102) = 2.12$, $p_{fdr} = .235$, partial $\eta^2 = .04$), and TP ($F(2, 99) = 2.59$, $p_{fdr} = .235$, partial $\eta^2 = .04$) ROIs. Figure 2 displays the covariate-adjusted, group-wise means of all sMRI outcomes and their 95% CIs. A summary of all ANCOVA models predicting sMRI outcomes can be found in Table 2.

Predicting task outcomes through proteinopathy and structural atrophy

In the whole sample, Braak I/II ROI tau SUVr significantly explained variance in *Pr*s in the object condition ($n = 113$, $F(5, 108) = 30.16$, $R^2_{adj.} = .51$, $b = –0.11$, $\beta = –.021$, $p_{fdr} = .007$). There was no effect of tau SUVr signal on *Pr*s in the scene condition ($n = 111$, $F(5,$

Figure 3

*Associations of object-specific (**A**, **B**) and scene-specific (**C**, **D**) mnemonic discrimination with Braak I/II ROI tau SUVr (**A**, **C**) and early Aβ ROI SUVr (**B**, **D**) in the whole sample.*

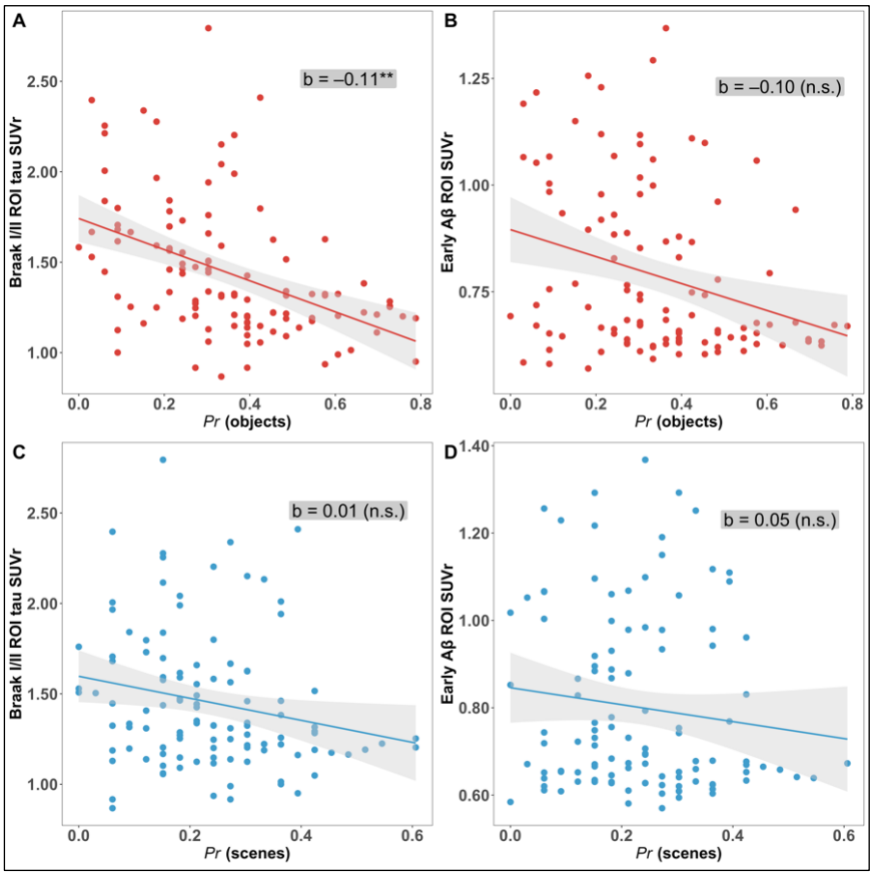

Note. The displayed coefficients b are adjusted for age, sex, and years of education. **A** $n = 113$, $F(5, 108) = 30.16$, $R^2_{adj.}$. =.51, b= –0.11, β=–.021, p_{fdr} =.007). **B** $n = 111$, F(5,106)=25.60, $R^2_{adj.}$ =.47,b = –0.10, β=0.04, $p_{fdr} = .629$. **C** $n = 113$, $F(5, 108) = 14.38$, $R^2_{adj.} = .32$, b = 0.01, β = –0.09, $p_{fdr} < .369$. **D** $n = 113$, $F(5, 108) = 14.18$, $R^2_{adj.} = .32$, b = 0.05, β = –0.14, $p_{fdr} = .321$). ** $p_{fdr} < .01$. SUVr = standardised uptake value ratio. ROI = region of interest.

106) = 25.60, $R^2_{adj.}$ = .47, *b* = –0.10, β = 0.04, p_{fdr} = .629), or on *Br*s in the object (*n* = 113, F(5, 108) = 14.38, $R^2_{adj.}$ = .32, *b* = 0.01, β = –0.09, p_{fdr} < .369) and scene condition (*n* = 113, F(5, 108) = 14.18, $R^2_{adj.}$ = .32, *b* = 0.05, β = –0.14, p_{fdr} = .321). Early Aβ ROI SUVr and sMRI outcomes did not contribute significantly to the prediction of task outcomes. The relationships of PET outcomes and *Pr*s are visualized Figure 3. Overviews of all multiple linear regression models are provided in Tables A2–A17 of the Appendix.

Mediation effects of sMRI measures on the relationship of Aβ and tau PET signal with task outcomes

Due to the lack of significant associations of sMRI and task outcomes, no mediation analyses were run.

Discussion

In the present study, I used a mnemonic discrimination task, ROI-based sMRI, as well as Aβ and tau PET to explore the trajectories and relationships of domain-specific episodic memory, regional atrophy, and proteinopathy in early stages of AD. There was no statistically significant evidence of different trajectories in object- compared to scene-based memory. However, there was a trend of lower object discrimination in the MCI Aβ+ group compared to the CU groups. For scene-based mnemonic discrimination as well as object- and scene-specific response bias, relatively stable outcomes could be observed across diagnostic groups. Participants with AD-related MCI had smaller CA2/3 GMVs compared to CU Aβ+ and CU Aβ- participants. Trends towards smaller GMVs in the MCI Aβ+ group compared to the two CU groups were observed for all other hippocampal subfields. Aside from an association of tau PET signal and object-based mnemonic discrimination in the whole sample, I found no

significant predictions of domain-specific mnemonic discrimination or response bias by measures of regional atrophy or early Aβ and tau burden.

Given the trend of lower object discrimination in the MCI Aβ+ group compared to the CU groups, my findings suggest that on the AD continuum, cognitive decline might occur first in object-based processing before it affects scene-based processing. As this trend is driven by low object discrimination in the MCI Aβ+ group, it is likely that the interaction effect of diagnostic group and domain did not reach statistical significance due to the low sample size in this specific group. Generally, this trend is in line with previous studies suggesting a greater vulnerability of the AT than the PM system to cognitive losses due to normal ageing (Reagh et al., 2016; Stark & Stark, 2017) and AD (Berron et al., 2019; Didic et al., 2011; Fidalgo et al., 2016). I also observed a negative relationship of early tau, but not Aβ, burden with object-based mnemonic discrimination in the whole sample. This result corresponds to a study by Berron et al. (2019), who showed declining object- but not scene-based mnemonic discrimination with increasing CSF p-tau and t-tau in a sample of healthy older adults and AD patients. Here, associations of CSF $A\beta_{42}/A\beta_{40}$ ratio were found neither for object- nor scene-specific mnemonic discrimination. While only few studies have investigated the distinct effects of Aβ and tau pathology on domain-specific episodic memory, a larger body of research has focused on their impact on global cognition. Supporting my findings of tau-related cognitive decline, it has been proposed that cognitive impairment cannot be explained by Aβ alone but requires the presence of tau as a driving force (Jack et al., 2019; Soldan et al., 2016; Sperling et al., 2019). In fact, it has been reported that local tau is related to region-specific cognition in older adults with AD-related MCI or AD dementia (e.g., tau PET signal in the left temporal lobes being negatively related to semantic memory; Bejanin et al., 2017). Given these findings, the question arises if a local impact of tau pathology on cognition can be observed independently in the PM and AT

systems. So far, this effect has been shown in only one sample (Maass et al., 2019) and will have to be replicated elsewhere. Notably, the authors also found a negative association of local Aβ burden in the PM system with scene-based mnemonic discrimination, which I could not observe in my data. However, the effect of PM Aβ on scene-based mnemonic discrimination reported by Maass et al. was considerably weaker than the effect of local AT tau on object-based mnemonic discrimination. Aβ might still impact scene-based episodic memory before an object-specific cognitive decline occurs. If this is the case, the effect is probably extremely small and requires larger sample sizes and/or more sensitive methods. It is also important to consider that, in the present study, mnemonic discrimination performance was less varied in scene condition compared to object condition. Thus, differences in scene-based mnemonic discrimination may have required higher statistical power to be detected. Moreover, I found that across all groups, discrimination performance was lower in the scene condition compared to the object condition. Thus, floor effects may have concealed group differences in scene-based mnemonic discrimination.

Surprisingly, the only significant difference between diagnostic groups in regional atrophy was found in the hippocampal CA2/3 subfield. Lower CA2/3 GMV in MCI patients with abnormal Aβ has been described elsewhere (Wisse et al., 2014). However, the majority of studies investigating structural integrity of hippocampal subfields over the course of AD support the notion of atrophy first emerging in CA1 and Sub before other subfields are subsequently affected (de Flores et al., 2015). This spatiotemporal order of atrophy is plausible given that among hippocampal subfields, CA1 is the earliest to be affected by tau (Lace et al., 2009) and that tau has been associated with subsequent local atrophy (La Joie et al., 2020; Xie et al., 2020). While higher vulnerability of CA1 and Sub to AD-related neurodegeneration was not reflected in my data, it is important to note that trends of smaller GMV in MCI Aβ+ individuals could be observed across all subfields, and not just CA2/3.

These trends not reaching statistical significance may be due to the small size of the MCI Aβ+ group (i.e., the group that exhibited highest tau PET signal and might thus be most prone to neurodegeneration) as well as the fact that the chosen statistical analyses required impactful statistical corrections for multiple comparisons. Generally, my data shows a trend of AD-related regional atrophy first occurring in the hippocampus before other cortical regions are affected. This is in line with previous research (Jagust, 2018).

Moreover, I found trends of larger hippocampal subfield GMVs in the CU Aβ+ group compared to the CU Aβ- group. This tendency is in line with some previous reports of non-linear relationships of Aβ burden and hippocampal subfield volumes. For instance, Müller-Ehrenberg et al. (2018) showed quadratic relationships of subfield (CA1-4, DG, Sub) GMVs and CSF $A\beta_{42}$ levels in a sample including demented and non-demented older adults from the Alzheimer's Disease Neuroimaging Initiative cohort. Such non-linear effects have been shown for cortical thickness in a cross-sectional (Fortea et al., 2011, 2014; Montal et al., 2018) but also longitudinal (Pegueroles et al., 2017) studies. Montal et al. (2021) suggest that Aβ initially drives an increase in cortical thickness and a decrease in cortical diffusivity already about 20 years before symptom onset. When tau starts becoming abnormal, Montal et al. propose that the two proteinopathies interact, resulting in cortical thinning and increased cortical diffusivity.

I did not find evidence of domain-specific episodic memory being related to regional atrophy in the MTL as well as the PM and AT systems. If not related to structural losses, is possible that domain-specific memory decline in early AD is instead linked to decreasing functional integrity. This assumption is plausible, especially in the light of previous studies showing the detrimental effect of tau on resting-state and task-based markers of functional integrity (Adams et al., 2021; Franzmeier et al., 2019, 2020; Maass et al., 2019). Additionally, recent studies suggested memory impairment to be primarily driven by tau-

related functional alterations in CU before the relationship of tau and memory is mediated by structural losses in MCI (Berron et al., 2020, 2021). If structural effects on cognition do not occur before the MCI stage of AD, it is likely that the present MCI Aβ group was too small to reflect this effect.

In the present study, no differences in AD diagnostic groups were found for domain-specific response bias. This contrasts previous studies reporting a more liberal response bias in AD patients compared to healthy controls (Budson et al., 2006; Deason et al., 2017; Russo et al., 2017). These studies did not assess AD biomarkers and were limited to comparisons of patients with MCI or AD dementia with healthy controls. Hence, my study is the first one to investigate if a more liberal response bias already occurs in CU individuals with abnormal Aβ and suggests that this is not the case. However, it might be that response bias was, to some degree, manipulated by the instruction to consider stimuli that show any slight modification as new. As a consequence, participants might have interpreted being unsure as a reason to respond "new". If this was the case, important variance in response bias may have been undermined. The rather high (i.e., liberal) response bias outcomes across all diagnostic groups support this explanation.

Limitations and future directions

My study has several limitations. First, its cross-sectional design does not allow statements on the causal mechanisms and temporal sequences underlying events of structural atrophy and episodic memory loss along the AD continuum. Second, the statistical analyses led to a large number of multiple comparisons, increasing the likelihood of obtaining false positive results. In turn, the subsequent statistical corrections may have undermined small effects that exist in the population. Thus, the present study is not sufficient to make general claims. Further studies are necessary to specifically target the effects proposed here .Third,

the present study was likely underpowered for detecting effects that are specific to AD-related MCI. This limitation is particularly relevant as previous research has suggested that atrophy is related to cognitive decline in patient with MCI but not in CU individuals. Fourth, this study did not provide data on functional activation or connectivity, which both have been found to be related to cognition in CU, independently from atrophy. Finally, I tested domain-specific episodic memory only once during an MRI scan – a situation which was unfamiliar and potentially distressing to participants. The repeated assessment of cognitive function in familiar settings (e.g., via repeated mobile assessments) is a promising approach that enables researchers to run frequent assessments of cognitive function while achieving established psychometric standards (Sliwinski et al., 2018). Eventually, mobile assessment of cognitive function could facilitate the longitudinal monitoring of cognitive decline in AD. In combination with repeated biomarker assessments, such longitudinal studies should aim to disentangle the effects of structural and functional neuronal changes on domain-specific episodic memory as well as their occurrence relative to changes in different AD biomarkers. Ultimately, this approach could help identify markers of earliest cognitive decline due to AD.

Conclusion

In summary, my study found a tendency of AD-related cognitive decline first occurring in object-based processing while scene-based processing remained stable across groups of early AD patients and healthy CU individuals. Object-based episodic memory was negatively related to early tau but not Aβ burden which is in line with recent studies investigating the complex relationships of AD biomarkers and cognition. As I found no associations of regional atrophy and cognition, the present study is another piece of evidence suggesting an alternative mediating mechanism explaining cognitive decline in preclinical

and prodromal AD stages. Further studies are needed to test potential neuropathological processes causing early AD-related cognitive decline.

References

Adams, J. N., Maass, A., Berron, D., Harrison, T. M., Baker, S. L., Thomas, W. P., Stanfill, M., & Jagust, W. J. (2021). Reduced Repetition Suppression in Aging is Driven by Tau–Related Hyperactivity in Medial Temporal Lobe. *The Journal of Neuroscience*, *41*(17), 3917–3931. https://doi.org/10.1523/JNEUROSCI.2504-20.2021

Agster, K. L., & Burwell, R. D. (2013). Hippocampal and subicular efferents and afferents of the perirhinal, postrhinal, and entorhinal cortices of the rat. *Behavioural Brain Research*, *254*, 50–64. https://doi.org/10.1016/j.bbr.2013.07.005

Altman, N., & Krzywinski, M. (2016). Analyzing outliers: Influential or nuisance? *Nature Methods*, *13*(4), 281–282. https://doi.org/10.1038/nmeth.3812

American Psychiatric Association. (2013). *Diagnostic and statistical manual of mental disorders: DSM-5* (5th ed., pp. xliv, 947 p. ;). American Psychiatric Association Arlington, VA.

Baker, S. L., Maass, A., & Jagust, W. J. (2017). Considerations and code for partial volume correcting [18F]-AV-1451 tau PET data. *Data in Brief*, *15*, 648–657. https://doi.org/10.1016/j.dib.2017.10.024

Bejanin, A., Schonhaut, D. R., La Joie, R., Kramer, J. H., Baker, S. L., Sosa, N., Ayakta, N., Cantwell, A., Janabi, M., Lauriola, M., O'Neil, J. P., Gorno-Tempini, M. L., Miller, Z. A., Rosen, H. J., Miller, B. L., Jagust, W. J., & Rabinovici, G. D. (2017). Tau pathology and neurodegeneration contribute to cognitive impairment in Alzheimer's disease. *Brain: A Journal of Neurology*, *140*(12), 3286–3300. https://doi.org/10.1093/brain/awx243

Berron, D., Cardenas-Blanco, A., Bittner, D., Metzger, C. D., Spottke, A., Heneka, M. T., Fliessbach, K., Schneider, A., Teipel, S. J., Wagner, M., Speck, O., Jessen, F., & Düzel, E. (2019). Higher CSF Tau Levels Are Related to Hippocampal Hyperactivity and Object Mnemonic Discrimination in Older Adults. *Journal of Neuroscience*, *39*(44), 8788–8797. https://doi.org/10.1523/JNEUROSCI.1279-19.2019

Berron, D., Neumann, K., Maass, A., Schütze, H., Fliessbach, K., Kiven, V., Jessen, F., Sauvage, M., Kumaran, D., & Düzel, E. (2018). Age-related functional changes in domain-specific medial temporal lobe pathways. *Neurobiology of Aging*, *65*, 86–97. https://doi.org/10.1016/j.neurobiolaging.2017.12.030

Berron, D., van Westen, D., Ossenkoppele, R., Strandberg, O., & Hansson, O. (2020). Medial temporal lobe connectivity and its associations with cognition in early Alzheimer's disease. *Brain*, *143*(4), 1233–1248. https://doi.org/10.1093/brain/awaa068

Berron, D., Vogel, J. W., Insel, P. S., Pereira, J. B., Xie, L., Wisse, L. E. M., Yushkevich, P. A., Palmqvist, S., Mattsson-Carlgren, N., Stomrud, E., Smith, R., Strandberg, O., & Hansson, O. (2021). Early stages of tau pathology and its associations with functional connectivity, atrophy and memory. *Brain*, *114*. https://doi.org/10.1093/brain/awab114

Borlikova, G. G., Trejo, M., Mably, A. J., Mc Donald, J. M., Sala Frigerio, C., Regan, C. M., Murphy, K. J., Masliah, E., & Walsh, D. M. (2013). Alzheimer brain-derived amyloid β-protein impairs synaptic remodeling and memory consolidation. *Neurobiology of Aging*, *34*(5), 1315–1327. https://doi.org/10.1016/j.neurobiolaging.2012.10.028

Braak, H., & Braak, E. (1991). Neuropathological stageing of Alzheimer-related changes. *Acta Neuropathologica*, *82*(4), 239–259. https://doi.org/10.1007/BF00308809

Braak, H., & Del Tredici, K. (2012). Alzheimer's disease: Pathogenesis and prevention. *Alzheimer's & Dementia: The Journal of the Alzheimer's Association*, *8*(3), 227–233. https://doi.org/10.1016/j.jalz.2012.01.011

Budson, A. E., Wolk, D. A., Chong, H., & Waring, J. D. (2006). Episodic memory in Alzheimer's disease: Separating response bias from discrimination. *Neuropsychologia*, *44*(12), 2222–2232. https://doi.org/10.1016/j.neuropsychologia.2006.05.024

de Flores, R., La Joie, R., & Chételat, G. (2015). Structural imaging of hippocampal subfields in healthy aging and Alzheimer's disease. *Neuroscience*, *309*, 29–50. https://doi.org/10.1016/j.neuroscience.2015.08.033

Deason, R. G., Tat, M. J., Flannery, S., Mithal, P. S., Hussey, E. P., Crehan, E. T., Ally, B. A., & Budson, A. E. (2017). Response bias and response monitoring: Evidence from healthy older adults and patients with mild Alzheimer's disease. *Brain and Cognition*, *119*, 17–24. https://doi.org/10.1016/j.bandc.2017.09.002

Del Re, A. C. (2013). *compute.es: Compute effect sizes* [Manual]. https://cran.r-project.org/package=compute.es

Didic, M., Barbeau, E. J., Felician, O., Tramoni, E., Guedj, E., Poncet, M., & Ceccaldi, M. (2011). Which memory system is impaired first in Alzheimer's disease? *Journal of Alzheimer's Disease: JAD*, *27*(1), 11–22. https://doi.org/10.3233/JAD-2011-110557

Ding, S.-L., & Van Hoesen, G. W. (2010). Borders, extent, and topography of human perirhinal cortex as revealed using multiple modern neuroanatomical and pathological markers. *Human Brain Mapping*, *31*(9), 1359–1379. https://doi.org/10.1002/hbm.20940

Eichenbaum, H., Yonelinas, A. R., & Ranganath, C. (2007). The Medial Temporal Lobe and Recognition Memory. *Annual Review of Neuroscience*, *30*, 123–152. https://doi.org/10.1146/annurev.neuro.30.051606.094328

Fidalgo, C. O., Changoor, A. T., Page-Gould, E., Lee, A. C. H., & Barense, M. D. (2016). Early cognitive decline in older adults better predicts object than scene recognition performance. *Hippocampus*, *26*(12), 1579–1592. https://doi.org/10.1002/hipo.22658

Folstein, M. F., Folstein, S. E., & McHugh, P. R. (1975). "Mini-mental state": A practical method for grading the cognitive state of patients for the clinician. *Journal of Psychiatric Research*, *12*(3), 189–198. https://doi.org/10.1016/0022-3956(75)90026-6

Fortea, J., Sala-Llonch, R., Bartrés-Faz, D., Lladó, A., Solé-Padullés, C., Bosch, B., Antonell, A., Olives, J., Sanchez-Valle, R., Molinuevo, J. L., & Rami, L. (2011). Cognitively Preserved Subjects with Transitional Cerebrospinal Fluid ß-Amyloid 1-42 Values Have Thicker Cortex in Alzheimer's Disease Vulnerable Areas. *Biological Psychiatry*, *70*(2), 183–190. https://doi.org/10.1016/j.biopsych.2011.02.017

Fortea, J., Vilaplana, E., Alcolea, D., Carmona-Iragui, M., Sánchez-Saudinos, M.-B., Sala, I., Antón-Aguirre, S., González, S., Medrano, S., Pegueroles, J., Morenas, E., Clarimón, J., Blesa, R., & Lleó, A. (2014). Cerebrospinal fluid β-amyloid and phospho-tau biomarker interactions affecting brain structure in preclinical Alzheimer disease. *Annals of Neurology*, *76*(2), 223–230. https://doi.org/10.1002/ana.24186

Fox, J., & Weisberg, S. (2019). *An R companion to applied regression* (3rd ed.). Sage. https://socialsciences.mcmaster.ca/jfox/Books/Companion/

Franzmeier, N., Neitzel, J., Rubinski, A., Smith, R., Strandberg, O., Ossenkoppele, R., Hansson, O., & Ewers, M. (2020). Functional brain architecture is associated with the rate of tau accumulation in Alzheimer's disease. *Nature Communications*, *11*(1), 347. https://doi.org/10.1038/s41467-019-14159-1

Franzmeier, N., Rubinski, A., Neitzel, J., Kim, Y., Damm, A., Na, D. L., Kim, H. J., Lyoo, C. H., Cho, H., Finsterwalder, S., Duering, M., Seo, S. W., & Ewers, M. (2019).

Functional connectivity associated with tau levels in ageing, Alzheimer's, and small vessel disease. *Brain*, *142*(4), 1093–1107. https://doi.org/10.1093/brain/awz026

Freir, D. B., Fedriani, R., Scully, D., Smith, I. M., Selkoe, D. J., Walsh, D. M., & Regan, C. M. (2011). Aβ oligomers inhibit synapse remodelling necessary for memory consolidation. *Neurobiology of Aging*, *32*(12), 2211–2218. https://doi.org/10.1016/j.neurobiolaging.2010.01.001

Golby, A., Silverberg, G., Race, E., Gabrieli, S., O'Shea, J., Knierim, K., Stebbins, G., & Gabrieli, J. (2005). Memory encoding in Alzheimer's disease: An fMRI study of explicit and implicit memory. *Brain*, *128*(4), 773–787. https://doi.org/10.1093/brain/awh400

Hothorn, T., Bretz, F., & Westfall, P. (2008). Simultaneous inference in general parametric models. *Biometrical Journal*, *50*(3), 346–363.

Inhoff, M. C., & Ranganath, C. (2017). Dynamic cortico-hippocampal networks underlying memory and cognition: The PMAT framework. In *The hippocampus from cells to systems: Structure, connectivity, and functional contributions to memory and flexible cognition* (pp. 559–589). Springer International Publishing AG. https://doi.org/10.1007/978-3-319-50406-3_18

Jack, C. R., Bennett, D. A., Blennow, K., Carrillo, M. C., Dunn, B., Haeberlein, S. B., Holtzman, D. M., Jagust, W., Jessen, F., Karlawish, J., Liu, E., Molinuevo, J. L., Montine, T., Phelps, C., Rankin, K. P., Rowe, C. C., Scheltens, P., Siemers, E., Snyder, H. M., … Silverberg, N. (2018). NIA-AA Research Framework: Toward a biological definition of Alzheimer's disease. *Alzheimer's & Dementia*, *14*(4), 535–562. https://doi.org/10.1016/j.jalz.2018.02.018

Jack, C. R., Jr, Lowe, V. J., Weigand, S. D., Wiste, H. J., Senjem, M. L., Knopman, D. S., Shiung, M. M., Gunter, J. L., Boeve, B. F., Kemp, B. J., Weiner, M., Petersen, R. C.,

& the Alzheimer's Disease Neuroimaging Initiative. (2009). Serial PIB and MRI in normal, mild cognitive impairment and Alzheimer's disease: Implications for sequence of pathological events in Alzheimer's disease. *Brain*, *132*(5), 1355–1365. https://doi.org/10.1093/brain/awp062

Jack, C. R., Wiste, H. J., Botha, H., Weigand, S. D., Therneau, T. M., Knopman, D. S., Graff-Radford, J., Jones, D. T., Ferman, T. J., Boeve, B. F., Kantarci, K., Lowe, V. J., Vemuri, P., Mielke, M. M., Fields, J. A., Machulda, M. M., Schwarz, C. G., Senjem, M. L., Gunter, J. L., & Petersen, R. C. (2019). The bivariate distribution of amyloid-β and tau: Relationship with established neurocognitive clinical syndromes. *Brain*, *142*(10), 3230–3242. https://doi.org/10.1093/brain/awz268

Jagust, W. (2018). Imaging the evolution and pathophysiology of Alzheimer disease. *Nature Reviews Neuroscience*, *19*(11), 687–700. https://doi.org/10.1038/s41583-018-0067-3

Jansen, W. J., Ossenkoppele, R., Knol, D. L., Tijms, B. M., Scheltens, P., Verhey, F. R. J., Visser, P. J., & and the Amyloid Biomarker Study Group. (2015). Prevalence of Cerebral Amyloid Pathology in Persons Without Dementia: A Meta-analysis. *JAMA*, *313*(19), 1924–1938. https://doi.org/10.1001/jama.2015.4668

Kaplan, E., Goodglass, H., & Weintraub, S. (2001). *The Boston Naming Test* (2nd ed.). Lippincott Williams & Wilkins.

La Joie, R., Visani, A. V., Baker, S. L., Brown, J. A., Bourakova, V., Cha, J., Chaudhary, K., Edwards, L., Iaccarino, L., Janabi, M., Lesman-Segev, O. H., Miller, Z. A., Perry, D. C., O'Neil, J. P., Pham, J., Rojas, J. C., Rosen, H. J., Seeley, W. W., Tsai, R. M., … Rabinovici, G. D. (2020). Prospective longitudinal atrophy in Alzheimer's disease correlates with the intensity and topography of baseline tau-PET. *Science Translational Medicine*, *12*(524). https://doi.org/10.1126/scitranslmed.aau5732

Lace, G., Savva, G. M., Forster, G., de Silva, R., Brayne, C., Matthews, F. E., Barclay, J. J., Dakin, L., Ince, P. G., Wharton, S. B., & on behalf of MRC-CFAS. (2009). Hippocampal tau pathology is related to neuroanatomical connections: An ageing population-based study. *Brain*, *132*(5), 1324–1334. https://doi.org/10.1093/brain/awp059

Libby, L. A., Hannula, D. E., & Ranganath, C. (2014). Medial temporal lobe coding of item and spatial information during relational binding in working memory. *The Journal of Neuroscience*, *34*(43), 14233–14242. https://doi.org/10.1523/JNEUROSCI.0655-14.2014

Maass, A., Berron, D., Harrison, T. M., Adams, J. N., La Joie, R., Baker, S., Mellinger, T., Bell, R. K., Swinnerton, K., Inglis, B., Rabinovici, G. D., Düzel, E., & Jagust, W. J. (2019). Alzheimer's pathology targets distinct memory networks in the ageing brain. *Brain*, *142*(8), 2492–2509. https://doi.org/10.1093/brain/awz154

Mohs, R. C. (1996). The Alzheimer's Disease Assessment Scale. *International Psychogeriatrics*, *8*(2), 195–203. https://doi.org/10.1017/s1041610296002578

Montal, V., Vilaplana, E., Alcolea, D., Pegueroles, J., Pasternak, O., González-Ortiz, S., Clarimón, J., Carmona-Iragui, M., Illán-Gala, I., Morenas-Rodríguez, E., Ribosa-Nogué, R., Sala, I., Sánchez-Saudinós, M.-B., García-Sebastian, M., Villanúa, J., Izagirre, A., Estanga, A., Ecay-Torres, M., Iriondo, A., … Fortea, J. (2018). Cortical microstructural changes along the Alzheimer's disease continuum. *Alzheimer's & Dementia: The Journal of the Alzheimer's Association*, *14*(3), 340–351. https://doi.org/10.1016/j.jalz.2017.09.013

Montal, V., Vilaplana, E., Pegueroles, J., Bejanin, A., Alcolea, D., Carmona-Iragui, M., Clarimón, J., Levin, J., Cruchaga, C., Graff-Radford, N. R., Noble, J. M., Lee, J.-H., Allegri, R., Karch, C. M., Laske, C., Schofield, P. R., Salloway, S., Ances, B.,

Benzinger, T., … Fortea, J. (2021). Biphasic cortical macro- and microstructural changes in autosomal dominant Alzheimer's disease. *Alzheimer's & Dementia*, *17*(4), 618–628. https://doi.org/10.1002/alz.12224

Mormino, E. C., Kluth, J. T., Madison, C. M., Rabinovici, G. D., Baker, S. L., Miller, B. L., Koeppe, R. A., Mathis, C. A., Weiner, M. W., Jagust, W. J., & the Alzheimer's Disease Neuroimaging Initiative*. (2009). Episodic memory loss is related to hippocampal-mediated β-amyloid deposition in elderly subjects. *Brain*, *132*(5), 1310–1323. https://doi.org/10.1093/brain/awn320

Müller-Ehrenberg, L., Riphagen, J. M., Verhey, F. R. J., Sack, A. T., Jacobs, H. I. L., & Alzheimer's Disease Neuroimaging Initiative. (2018). Alzheimer's Disease Biomarkers Have Distinct Associations with Specific Hippocampal Subfield Volumes. *Journal of Alzheimer's Disease: JAD*, *66*(2), 811–823. https://doi.org/10.3233/JAD-180676

Murphy, K. J., Troyer, A. K., Levine, B., & Moscovitch, M. (2008). Episodic, but not semantic, autobiographical memory is reduced in amnestic mild cognitive impairment. *Neuropsychologia*, *46*(13), 3116–3123. https://doi.org/10.1016/j.neuropsychologia.2008.07.004

Navarro, D. (2015). *Learning statistics with R: A tutorial for psychology students and other beginners. (Version 0.5)* [Manual]. http://ua.edu.au/ccs/teaching/lsr

Neunuebel, J. P., & Knierim, J. J. (2014). CA3 Retrieves Coherent Representations from Degraded Input: Direct Evidence for CA3 Pattern Completion and Dentate Gyrus Pattern Separation. *Neuron*, *81*(2), 416–427. https://doi.org/10.1016/j.neuron.2013.11.017

Ossenkoppele, R., Rabinovici, G. D., Smith, R., Cho, H., Schöll, M., Strandberg, O., Palmqvist, S., Mattsson, N., Janelidze, S., Santillo, A., Ohlsson, T., Jögi, J., Tsai, R.,

La Joie, R., Kramer, J., Boxer, A. L., Gorno-Tempini, M. L., Miller, B. L., Choi, J. Y., … Hansson, O. (2018). Discriminative Accuracy of [18F]flortaucipir Positron Emission Tomography for Alzheimer Disease vs Other Neurodegenerative Disorders. *JAMA*, *320*(11), 1151–1162. https://doi.org/10.1001/jama.2018.12917

Palmqvist, S., Schöll, M., Strandberg, O., Mattsson, N., Stomrud, E., Zetterberg, H., Blennow, K., Landau, S., Jagust, W., & Hansson, O. (2017). Earliest accumulation of β-amyloid occurs within the default-mode network and concurrently affects brain connectivity. *Nature Communications*, *8*. https://doi.org/10.1038/s41467-017-01150-x

Pascoal, T. A., Therriault, J., Benedet, A. L., Savard, M., Lussier, F. Z., Chamoun, M., Tissot, C., Qureshi, M. N. I., Kang, M. S., Mathotaarachchi, S., Stevenson, J., Hopewell, R., Massarweh, G., Soucy, J.-P., Gauthier, S., & Rosa-Neto, P. (2020). 18F-MK-6240 PET for early and late detection of neurofibrillary tangles. *Brain*, *143*(9), 2818–2830. https://doi.org/10.1093/brain/awaa180

Pegueroles, J., Vilaplana, E., Montal, V., Sampedro, F., Alcolea, D., Carmona-Iragui, M., Clarimon, J., Blesa, R., Lleó, A., & Fortea, J. (2017). Longitudinal brain structural changes in preclinical Alzheimer's disease. *Alzheimer's & Dementia*, *13*(5), 499–509. https://doi.org/10.1016/j.jalz.2016.08.010

R Core Team. (2021). *R: A language and environment for statistical computing* [Manual]. https://www.R-project.org/

Ravikumar, S., Wisse, L. E. M., Ittyerah, R., Lim, S., Lavery, M., Xie, L., Robinson, J. L., Schuck, T., Grossman, M., Lee, E. B., Tisdall, M. D., Prabhakaran, K., Detre, J. A., Das, S. R., Mizsei, G., Artacho-Pérula, E., de Onzono Martin, M. M. I., del Mar Arroyo Jiménez, M., Muñoz, M., … Yushkevich, P. A. (2020). Building an Ex Vivo Atlas of the Earliest Brain Regions Affected by Alzheimer's Disease Pathology. *2020*

IEEE 17th International Symposium on Biomedical Imaging (ISBI), 113–117. https://doi.org/10.1109/ISBI45749.2020.9098427

Reagh, Z. M., Ho, H. D., Leal, S. L., Noche, J. A., Chun, A., Murray, E. A., & Yassa, M. A. (2016). Greater loss of object than spatial mnemonic discrimination in aged adults. *Hippocampus*, *26*(4), 417–422. https://doi.org/10.1002/hipo.22562

Reitan, R. M. (1955). The relation of the Trail Making Test to organic brain damage. *Journal of Consulting Psychology*, *19*(5), 393–394. https://doi.org/10.1037/h0044509

Ritchey, M., Libby, L. A., & Ranganath, C. (2015). Chapter 3 - Cortico-hippocampal systems involved in memory and cognition: The PMAT framework. In S. O'Mara & M. Tsanov (Eds.), *Progress in Brain Research* (Vol. 219, pp. 45–64). Elsevier. https://doi.org/10.1016/bs.pbr.2015.04.001

Russo, M. J., Cohen, G., Campos, J., Martin, M. E., Clarens, M. F., Sabe, L., Barcelo, E., & Allegri, R. F. (2017). Usefulness of Discriminability and Response Bias Indices for the Evaluation of Recognition Memory in Mild Cognitive Impairment and Alzheimer Disease. *Dementia and Geriatric Cognitive Disorders*, *43*(1–2), 1–14. https://doi.org/10.1159/000452255

Schöll, M., Lockhart, S. N., Schonhaut, D. R., O'Neil, J. P., Janabi, M., Ossenkoppele, R., Baker, S. L., Vogel, J. W., Faria, J., Schwimmer, H. D., Rabinovici, G. D., & Jagust, W. J. (2016). PET imaging of tau deposition in the aging human brain. *Neuron*, *89*(5), 971–982. https://doi.org/10.1016/j.neuron.2016.01.028

Schwarz, A. J., Yu, P., Miller, B. B., Shcherbinin, S., Dickson, J., Navitsky, M., Joshi, A. D., Devous, M. D., & Mintun, M. S. (2016). Regional profiles of the candidate tau PET ligand 18F-AV-1451 recapitulate key features of Braak histopathological stages. *Brain: A Journal of Neurology*, *139*(Pt 5), 1539–1550. https://doi.org/10.1093/brain/aww023

Sliwinski, M. J., Mogle, J. A., Hyun, J., Munoz, E., Smyth, J. M., & Lipton, R. B. (2018). Reliability and Validity of Ambulatory Cognitive Assessments. *Assessment*, *25*(1), 14–30. https://doi.org/10.1177/1073191116643164

Smith, A. (1982). *Symbol Digit Modalities Test Manual-Revised*. Western Psychological Services.

Snodgrass, J. G., & Corwin, J. (1988). Pragmatics of measuring recognition memory: Applications to dementia and amnesia. *Journal of Experimental Psychology: General*, *117*(1), 34–50. https://doi.org/10.1037/0096-3445.117.1.34

Soldan, A., Pettigrew, C., Cai, Q., Wang, M.-C., Moghekar, A. R., O'Brien, R. J., Selnes, O. A., Albert, M. S., & BIOCARD Research Team. (2016). Hypothetical Preclinical Alzheimer Disease Groups and Longitudinal Cognitive Change. *JAMA Neurology*, *73*(6), 698–705. https://doi.org/10.1001/jamaneurol.2016.0194

Sperling, R. A., Bates, J. F., Chua, E. F., Cocchiarella, A. J., Rentz, D. M., Rosen, B. R., Schacter, D. L., & Albert, M. S. (2003). FMRI studies of associative encoding in young and elderly controls and mild Alzheimer's disease. *Journal of Neurology, Neurosurgery & Psychiatry*, *74*(1), 44–50. https://doi.org/10.1136/jnnp.74.1.44

Sperling, R. A., Mormino, E. C., Schultz, A. P., Betensky, R. A., Papp, K. V., Amariglio, R. E., Hanseeuw, B. J., Buckley, R., Chhatwal, J., Hedden, T., Marshall, G. A., Quiroz, Y. T., Donovan, N. J., Jackson, J., Gatchel, J. R., Rabin, J. S., Jacobs, H., Yang, H.-S., Properzi, M., … Johnson, K. A. (2019). The impact of amyloid-beta and tau on prospective cognitive decline in older individuals. *Annals of Neurology*, *85*(2), 181–193. https://doi.org/10.1002/ana.25395

Stark, S. M., & Stark, C. E. L. (2017). Age-related deficits in the mnemonic similarity task for objects and scenes. *Behavioural Brain Research*, *333*, 109–117. https://doi.org/10.1016/j.bbr.2017.06.049

Thurfjell, L., Lilja, J., Lundqvist, R., Buckley, C., Smith, A., Vandenberghe, R., & Sherwin, P. (2014). Automated Quantification of 18F-Flutemetamol PET Activity for Categorizing Scans as Negative or Positive for Brain Amyloid: Concordance with Visual Image Reads. *Journal of Nuclear Medicine*, *55*(10), 1623–1628. https://doi.org/10.2967/jnumed.114.142109

Tingley, D., Yamamoto, T., Hirose, K., Keele, L., & Imai, K. (2014). mediation: R Package for Causal Mediation Analysis. *Journal of Statistical Software*, *59*(1), 1–38. https://doi.org/10.18637/jss.v059.i05

Tulving, E. (1983). *Elements of Episodic Memory*. Oxford University Press.

van den Berg, E., Poos, J. M., Jiskoot, L. C., Heijnen, L. M., Franzen, S., Steketee, R. M. E., Meijboom, R., de Jong, F. J., Seelaar, H., van Swieten, J. C., & Papma, J. M. (2020). Differences in Discriminability and Response Bias on Rey Auditory Verbal Learning Test Delayed Recognition in Behavioral Variant Frontotemporal Dementia and Alzheimer's Disease. *Journal of the International Neuropsychological Society*, *26*(9), 918–926. https://doi.org/10.1017/S1355617720000375

Villeneuve, S., Rabinovici, G. D., Cohn-Sheehy, B. I., Madison, C., Ayakta, N., Ghosh, P. M., La Joie, R., Arthur-Bentil, S. K., Vogel, J. W., Marks, S. M., Lehmann, M., Rosen, H. J., Reed, B., Olichney, J., Boxer, A. L., Miller, B. L., Borys, E., Jin, L.-W., Huang, E. J., … Jagust, W. (2015). Existing Pittsburgh Compound-B positron emission tomography thresholds are too high: Statistical and pathological evaluation. *Brain*, *138*(7), 2020–2033. https://doi.org/10.1093/brain/awv112

Vogel, J. W., Young, A. L., Oxtoby, N. P., Smith, R., Ossenkoppele, R., Strandberg, O. T., La Joie, R., Aksman, L. M., Grothe, M. J., Iturria-Medina, Y., Pontecorvo, M. J., Devous, M. D., Rabinovici, G. D., Alexander, D. C., Lyoo, C. H., Evans, A. C., & Hansson, O. (2021). Four distinct trajectories of tau deposition identified in

Alzheimer's disease. *Nature Medicine*, 1–11. https://doi.org/10.1038/s41591-021-01309-6

Wang, H., Das, S. R., Suh, J. W., Altinay, M., Pluta, J., Craige, C., Avants, B., & Yushkevich, P. A. (2011). A learning-based wrapper method to correct systematic errors in automatic image segmentation: Consistently improved performance in hippocampus, cortex and brain segmentation. *NeuroImage*, *55*(3), 968–985. https://doi.org/10.1016/j.neuroimage.2011.01.006

Warrington, E. K., & James, M. (1991). *The visual object and space perception battery*. Thames Valley Test Company.

Wisse, L. E. M., Biessels, G. J., Heringa, S. M., Kuijf, H. J., Koek, D. (H.) L., Luijten, P. R., & Geerlings, M. I. (2014). Hippocampal subfield volumes at 7T in early Alzheimer's disease and normal aging. *Neurobiology of Aging*, *35*(9), 2039–2045. https://doi.org/10.1016/j.neurobiolaging.2014.02.021

Xie, L., Wisse, L. E. M., Das, S. R., Vergnet, N., Dong, M., Ittyerah, R., de Flores, R., Yushkevich, P. A., Wolk, D. A., & Alzheimer's Disease Neuroimaging Initiative. (2020). Longitudinal atrophy in early Braak regions in preclinical Alzheimer's disease. *Human Brain Mapping*, *41*(16), 4704–4717. https://doi.org/10.1002/hbm.25151

Yassa, M. A., & Stark, C. E. L. (2011). Pattern separation in the hippocampus. *Trends in Neurosciences*, *34*(10), 515–525. https://doi.org/10.1016/j.tins.2011.06.006

Yushkevich, P. A., Pluta, J. B., Wang, H., Xie, L., Ding, S.-L., Gertje, E. C., Mancuso, L., Kliot, D., Das, S. R., & Wolk, D. A. (2015). Automated volumetry and regional thickness analysis of hippocampal subfields and medial temporal cortical structures in mild cognitive impairment. *Human Brain Mapping*, *36*(1), 258–287. https://doi.org/10.1002/hbm.22627

Appendix

Table A1

Characteristics of the ANCOVA subsample

	CU Aβ-	CU Aβ+	MCI Aβ+	Whole Sample
n	48	40	20	108
Females (%)	23 (47.92%)	20 (50.00%)	11 (55.00%)	54 (50.00%)
Age (SD)	68.90 (8.71)	71.47 (7.46)	73.70 (4.81)	70.74 (7.81)
Years of education (SD)	12.26 (3.02)	11.93 (3.02)	11.82 (4.22)	12.06 (3.24)
	0.35 (0.19)	0.37 (0.19)	0.19 (0.11)	0.33 (0.19)
Pr (objects) (SD)	0.23 (0.16)	0.23 (0.13)	0.17 (0.11)	0.22 (0.14)
Pr (scenes) (SD)	0.77 (0.23)	0.75 (0.21)	0.74 (0.26)	0.76 (0.23)
Br (objects) (SD)	0.73 (0.21)	0.74 (0.17)	0.73 (0.21)	0.74 (0.20)
Br (scenes) (SD)	0.64 (0.03)	0.92 (0.17)	1.01 (0.20)	0.82 (0.21)
	1.27 (0.20)	1.55 (0.40)	1.86 (0.38)	1.48 (0.39)
Early Aβ ROI SUVr (SD)	28.94 (1.17)	28.68 (1.38)	27.15 (2.03)	28.51 (1.57)
Braak I/II tau SUVr (SD)	2.88 (1.90)	3.35 (1.86)	6.65 (2.60)	3.75 (2.45)
	40.65 (9.82)	37.82 (9.38)	28.00 (8.52)	37.34 (10.41)
MMSE (SD)	23.42 (6.16)	22.25 (6.18)	14.10 (5.58)	21.26 (6.94)
ADAS delayed word recall (SD)	2.62 (1.81)	3.32 (1.85)	6.65 (2.60)	3.52 (2.43)
Symbol Digit Modalities Test (SD)	43.53 (11.73)	38.62 (10.57)	28.00 (8.52)	39.40 (12.11)
Animal fluency (SD)	24.50 (6.43)	22.37 (6.15)	14.10 (5.58)	22.06 (7.17)

Note. ADAS = Alzheimer's Disease Assessment Scale. Aβ = amyloid-β. CU = cognitively unimpaired. MCI = mild cognitive impairment. ROI = region of interest. SD = standard deviation. SUVr = standardized uptake value ratio.

Table A2

Pr (objects) predicted by PET and sMRI measures in the whole sample

IV	Model statistics				Coefficients							
					Age		Sex (female)		Years of education		IV	
	n (excl.)	*F*	*p*	$R^2_{adj.}$	β	p_{fdr}	β	p_{fdr}	β	p_{fdr}	β	p_{fdr}
Early Aβ ROI SUVr (SD)	111 (9)	25.60 (5, 106)	<.001***	0.47	-0.56	<.001***	0.19	.015*	-0.12	.095	-0.10	.341
Braak I/II tau SUVr (SD)	113 (8)	30.16 (5, 108)	<.001***	0.51	-0.51	<.001***	0.18	.015*	-0.12	.069	-0.21	.007**
CA1 $GMV_{adj.}$ (mm^3)	114 (7)	25.91 (5, 109)	<.001***	0.47	-0.55	<.001***	0.18	.017*	-0.10	.177	0.11	.634
CA2/3 $GMV_{adj.}$ (mm^3)	115 (6)	24.84 (5, 110)	<.001***	0.46	-0.54	<.001***	0.18	.019*	-0.12	.090	0.13	.634
DG $GMV_{adj.}$ (mm^3)	115 (6)	23.56 (5, 110)	<.001***	0.44	-0.57	<.001***	0.17	.025*	-0.13	.083	0.06	.717
Sub $GMV_{adj.}$ (mm^3)	113 (8)	23.31 (5, 108)	<.001***	0.44	-0.56	<.001***	0.16	.037*	-0.10	.178	0.07	.717
HT $GMV_{adj.}$ (mm^3)	113 (8)	22.71 (5, 108)	<.001***	0.44	-0.56	<.001***	0.18	.019*	-0.11	.146	0.04	.717
ErC thickness (mm)	112 (9)	21.83 (5, 107)	<.001***	0.43	-0.57	<.001***	0.17	.028*	-0.11	.171	0.03	.850
BA35 thickness (mm)	113 (8)	21.59 (5, 108)	<.001***	0.42	-0.52	<.001***	0.16	.041*	-0.11	.160	0.10	.538
BA36 thickness (mm)	113 (8)	21.82 (5, 108)	<.001***	0.43	-0.54	<.001***	0.19	.014*	-0.11	.157	0.05	.806
PhC thickness (mm)	114 (7)	22.38 (5, 109)	<.001***	0.43	-0.61	<.001***	0.17	.033*	-0.13	.087	-0.07	.687
IPC thickness (mm)	114 (7)	24.63 (5, 109)	<.001***	0.46	-0.50	<.001***	0.16	.036*	-0.15	.039*	0.14	.477
IsthCing thickness (mm)	114 (7)	23.58 (5, 109)	<.001***	0.44	-0.53	<.001***	0.20	.010*	-0.12	.105	0.09	.538
LOC thickness (mm)	113 (8)	27.42 (5, 108)	<.001***	0.49	-0.59	<.001***	0.17	.021*	-0.15	.029*	0.03	.850
mOFC thickness (mm)	114 (7)	26.35 (5, 109)	<.001***	0.47	-0.56	<.001***	0.17	.021*	-0.09	.207	0.13	.436
PCC thickness (mm)	115 (6)	25.16 (5, 110)	<.001***	0.46	-0.55	<.001***	0.18	.016*	-0.13	.060	0.14	.436
Prec thickness (mm)	114 (7)	25.47 (5, 109)	<.001***	0.46	-0.58	<.001***	0.18	.016*	-0.14	.048*	0.02	.865
ITC thickness (mm)	113 (8)	26.31 (5, 108)	<.001***	0.47	-0.53	<.001***	0.19	.013*	-0.11	.118	0.11	.538
lOFC thickness (mm)	115 (6)	25.48 (5, 110)	<.001***	0.46	-0.55	<.001***	0.19	.015*	-0.09	.210	0.16	.436
TP thickness (mm)	114 (7)	24.82 (5, 109)	<.001***	0.46	-0.54	<.001***	0.18	.017*	-0.13	.065	0.10	.538

Note. *** p_{fdr} < 001. **p_{fdr} < .01. *p_{fdr} < .05. Aβ = amyloid-β. BA = Brodmann area. CA = cornu ammonis. DG = dentate gyrus. ErC = entorhinal cortex. GMV = gray matter volume. HT = hippocampal tail. IPC = inferior parietal cortex. IsthCing = isthmus cingulate. ITC = inferior temporal cortex. IV = independent variable. LOC = lateral occipital cortex. lOFC = lateral orbitorfrontal cortex. mOFC = medial orbitorfrontal cortex. Sub = subiculum. TP = temporal pole. PCC = posterior cingulate cortex. PhC = parahippocampal cortex. Prec = Precuneus.

Table A3

Pr (scenes) predicted by PET and sMRI measures in the whole sample

IV	Model statistics				Coefficients							
					Age		Sex (female)		Years of education		Age	
	n (excl.)	*F*	*p*	n	*F*	p_{fdr}	n	*F*	β	n	*F*	p_{fdr}
Early Aβ ROI SUVr (SD)	113 (7)	14.18 (5, 108)	<.001***	0.32	-0.56	<.001***	0.10	.245	-0.09	.277	0.07	.399
Braak I/II tau SUVr (SD)	113 (8)	14.38 (5, 108)	<.001***	0.32	-0.57	<.001***	0.07	.376	-0.11	.173	0.04	.629
CA1 $GMV_{adj.}$ (mm^3)	114 (7)	14.23 (5, 109)	<.001***	0.32	-0.51	<.001***	0.09	.260	-0.08	.314	0.07	.717
CA2/3 $GMV_{adj.}$ (mm^3)	115 (6)	14.76 (5, 110)	<.001***	0.33	-0.54	<.001***	0.12	.148	-0.10	.186	-0.05	.717
DG $GMV_{adj.}$ (mm^3)	114 (7)	13.96 (5, 109)	<.001***	0.31	-0.51	<.001***	0.12	.144	-0.12	.126	0.04	.717
Sub $GMV_{adj.}$ (mm^3)	113 (8)	13.73 (5, 108)	<.001***	0.31	-0.49	<.001***	0.10	.253	-0.06	.438	0.09	.717
HT $GMV_{adj.}$ (mm^3)	114 (7)	13.99 (5, 109)	<.001***	0.31	-0.54	<.001***	0.10	.242	-0.09	.269	-0.01	.914
ErC thickness (mm)	113 (8)	13.33 (5, 108)	<.001***	0.31	-0.53	<.001***	0.10	.238	-0.07	.422	0.01	.931
BA35 thickness (mm)	113 (8)	14.12 (5, 108)	<.001***	0.32	-0.51	<.001***	0.13	.118	-0.08	.324	0.03	.850
BA36 thickness (mm)	114 (7)	14.01 (5, 109)	<.001***	0.32	-0.53	<.001***	0.13	.136	-0.10	.240	-0.04	.850
PhC thickness (mm)	115 (6)	14.78 (5, 110)	<.001***	0.33	-0.50	<.001***	0.12	.167	-0.10	.221	0.06	.806
IPC thickness (mm)	111 (10)	14.69 (5, 106)	<.001***	0.33	-0.39	<.001***	0.15	.073	-0.08	.325	0.18	.436
IsthCing thickness (mm)	113 (8)	13.61 (5, 108)	<.001***	0.31	-0.48	<.001***	0.12	.155	-0.11	.177	0.08	.686
LOC thickness (mm)	112 (9)	12.39 (5, 107)	<.001***	0.29	-0.51	<.001***	0.10	.269	-0.09	.292	0.02	.871
mOFC thickness (mm)	113 (8)	12.59 (5, 108)	<.001***	0.29	-0.47	<.001***	0.11	.213	-0.07	.376	0.10	.538
PCC thickness (mm)	113 (8)	15.75 (5, 108)	<.001***	0.35	-0.51	<.001***	0.11	.182	-0.11	.172	0.15	.436
Prec thickness (mm)	113 (8)	13.63 (5, 108)	<.001***	0.31	-0.49	<.001***	0.11	.200	-0.07	.360	0.08	.686
ITC thickness (mm)	114 (7)	13.99 (5, 109)	<.001***	0.32	-0.54	<.001***	0.10	.256	-0.09	.253	-0.02	.900
lOFC thickness (mm)	115 (6)	13.26 (5, 110)	<.001***	0.30	-0.48	<.001***	0.13	.116	-0.09	.284	0.10	.538
TP thickness (mm)	114 (7)	13.98 (5, 109)	<.001***	0.31	-0.53	<.001***	0.12	.137	-0.09	.279	-0.04	.850

Note. *** $p_{fdr} < 001$. ** $p_{fdr} < .01$. * $p_{fdr} < .05$. Aβ = amyloid-β. BA = Brodmann area. CA = cornu ammonis. DG = dentate gyrus. ErC = entorhinal cortex. GMV = gray matter volume. HT = hippocampal tail. IPC = inferior parietal cortex. IsthCing = isthmus cingulate. ITC = inferior temporal cortex. IV = independent variable. LOC = lateral occipital cortex. lOFC = lateral orbitorfrontal cortex. mOFC = medial orbitorfrontal cortex. Sub = subiculum. TP = temporal pole. PCC = posterior cingulate cortex. PhC = parahippocampal cortex. Prec = Precuneus.

Table A4

Br (objects) predicted by PET and sMRI measures in the whole sample

IV	Model statistics				Coefficients							
					Age		Sex (female)		Years of education		IV	
	n (excl.)	*F*	*p*	$R^2_{adj.}$	β	p_{fdr}	β	p_{fdr}	β	p_{fdr}	β	p_{fdr}
Early Aβ ROI SUVr (SD)	113 (7)	2.78 (5, 108)	.030**	0.06	0.14	.168	-0.20	.043*	0.09	.355	-0.15	.224
Braak I/II tau SUVr (SD)	112 (9)	2.38 (5, 107)	.056	0.05	0.12	.245	-0.19	.058	0.13	.180	-0.09	.369
CA1 $GMV_{adj.}$ (mm^3)	114 (7)	2.15 (5, 109)	.079	0.04	0.10	.324	-0.20	.043*	0.09	.316	0.04	.893
CA2/3 $GMV_{adj.}$ (mm^3)	114 (7)	2.11 (5, 109)	.085	0.04	0.08	.412	-0.20	.044*	0.09	.342	-0.01	.893
DG $GMV_{adj.}$ (mm^3)	113 (8)	2.61 (5, 108)	.040**	0.05	0.10	.298	-0.23	.021*	0.07	.463	-0.02	.893
Sub $GMV_{adj.}$ (mm^3)	112 (9)	2.58 (5, 107)	.042**	0.05	0.12	.253	-0.22	.030*	0.09	.315	0.04	.893
HT $GMV_{adj.}$ (mm^3)	113 (8)	2.16 (5, 108)	.078	0.04	0.11	.270	-0.18	.069	0.11	.239	0.05	.893
ErC thickness (mm)	114 (7)	2.13 (5, 109)	.082	0.04	0.09	.368	-0.20	.043*	0.10	.314	0.03	.976
BA35 thickness (mm)	113 (8)	1.83 (5, 108)	.129	0.03	0.07	.531	-0.20	.051	0.07	.491	-0.02	.976
BA36 thickness (mm)	111 (10)	3.63 (5, 106)	.008**	0.09	0.10	.332	-0.28	.005**	0.03	.791	-0.06	.976
PhC thickness (mm)	112 (9)	2.58 (5, 107)	.041**	0.05	0.12	.247	-0.22	.029*	0.09	.319	0.04	.976
IPC thickness (mm)	113 (8)	2.62 (5, 108)	.039**	0.05	0.11	.370	-0.23	.021*	0.06	.518	0.03	.976
IsthCing thickness (mm)	113 (8)	2.60 (5, 108)	.040**	0.05	0.09	.381	-0.24	.017*	0.06	.503	-0.01	.976
LOC thickness (mm)	113 (8)	2.67 (5, 108)	.036**	0.06	0.13	.226	-0.22	.035*	0.07	.436	0.06	.976
mOFC thickness (mm)	113 (8)	2.75 (5, 108)	.032**	0.06	0.07	.470	-0.24	.015*	0.05	.624	-0.07	.976
PCC thickness (mm)	113 (8)	15.75 (5, 108)	<.001***	0.35	-0.51	<.001***	0.11	.182	-0.11	.172	0.15	.436
Prec thickness (mm)	113 (8)	13.63 (5, 108)	<.001***	0.31	-0.49	<.001***	0.11	.200	-0.07	.360	0.08	.686
ITC thickness (mm)	114 (7)	13.99 (5, 109)	<.001***	0.32	-0.54	<.001***	0.10	.256	-0.09	.253	-0.02	.900
lOFC thickness (mm)	115 (6)	13.26 (5, 110)	<.001***	0.30	-0.48	<.001***	0.13	.116	-0.09	.284	0.10	.538
TP thickness (mm)	114 (7)	13.98 (5, 109)	<.001***	0.31	-0.53	<.001***	0.12	.137	-0.09	.279	-0.04	.850

Note. *** $p_{fdr} < 001$. ** $p_{fdr} < .01$. * $p_{fdr} < .05$. Aβ = amyloid-β. BA = Brodmann area. CA = cornu ammonis. DG = dentate gyrus. ErC = entorhinal cortex. GMV = gray matter volume. HT = hippocampal tail. IPC = inferior parietal cortex. IsthCing = isthmus cingulate. ITC = inferior temporal cortex. IV = independent variable. LOC = lateral occipital cortex. lOFC = lateral orbitorfrontal cortex. mOFC = medial orbitorfrontal cortex. Sub = subiculum. TP = temporal pole. PCC = posterior cingulate cortex. PhC = parahippocampal cortex. Prec = Precuneus.

Table A5

Br (scenes) predicted by PET and sMRI measures in the whole sample

IV	Model statistics				Coefficients							
					Age		Sex (female)		Years of education		IV	
	n (excl.)	*F*	*p*	$R^2_{adj.}$	β	p_{fdr}	β	p_{fdr}	β	p_{fdr}	β	p_{fdr}
Early Aβ ROI SUVr (SD)	114 (6)	1.15 (5, 109)	.337	0.01	0.03	.745	-0.16	.110	0.08	.404	-0.06	.539
Braak I/II tau SUVr (SD)	113 (8)	1.69 (5, 108)	.158	0.02	0.06	.594	-0.16	.116	0.12	.200	-0.14	.321
CA1 $GMV_{adj.}$ (mm^3)	115 (6)	1.09 (5, 110)	.366	0.00	0.00	.997	-0.16	.107	0.08	.397	-0.02	.893
CA2/3 $GMV_{adj.}$ (mm^3)	114 (7)	1.67 (5, 109)	.163	0.02	0.00	.997	-0.19	.061	0.10	.305	-0.07	.893
DG $GMV_{adj.}$ (mm^3)	114 (7)	1.70 (5, 109)	.156	0.02	0.01	.909	-0.19	.063	0.06	.498	-0.11	.893
Sub $GMV_{adj.}$ (mm^3)	111 (10)	1.57 (5, 106)	.189	0.02	0.10	.381	-0.16	.115	0.10	.317	0.16	.893
HT $GMV_{adj.}$ (mm^3)	114 (7)	1.09 (5, 109)	.367	0.00	0.00	.972	-0.13	.184	0.11	.239	-0.04	.893
ErC thickness (mm)	115 (6)	1.13 (5, 110)	.344	0.00	0.01	.923	-0.16	.101	0.10	.329	0.05	.976
BA35 thickness (mm)	114 (7)	1.55 (5, 109)	.194	0.02	-0.07	.532	-0.16	.113	0.06	.574	-0.14	.976
BA36 thickness (mm)	113 (8)	1.07 (5, 108)	.375	0.00	0.04	.659	-0.17	.099	0.05	.610	0.02	.976
PhC thickness (mm)	113 (8)	1.81 (5, 108)	.133	0.03	-0.04	.721	-0.13	.187	0.12	.213	-0.15	.976
IPC thickness (mm)	113 (8)	1.84 (5, 108)	.126	0.03	0.05	.705	-0.22	.032*	0.07	.445	0.03	.976
IsthCing thickness (mm)	114 (7)	1.58 (5, 109)	.186	0.02	0.04	.735	-0.19	.056	0.10	.312	0.04	.976
LOC thickness (mm)	114 (7)	1.34 (5, 109)	.259	0.01	0.03	.768	-0.19	.071	0.06	.512	0.02	.976
mOFC thickness (mm)	111 (10)	1.52 (5, 106)	.201	0.02	0.03	.777	-0.15	.155	0.05	.619	-0.12	.976
PCC thickness (mm)	113 (8)	15.75 (5, 108)	<.001***	0.35	-0.51	<.001***	0.11	.182	-0.11	.172	0.15	.436
Prec thickness (mm)	113 (8)	13.63 (5, 108)	<.001***	0.31	-0.49	<.001***	0.11	.200	-0.07	.360	0.08	.686
ITC thickness (mm)	114 (7)	13.99 (5, 109)	<.001***	0.32	-0.54	<.001***	0.10	.256	-0.09	.253	-0.02	.900
lOFC thickness (mm)	115 (6)	13.26 (5, 110)	<.001***	0.30	-0.48	<.001***	0.13	.116	-0.09	.284	0.10	.538
TP thickness (mm)	114 (7)	13.98 (5, 109)	<.001***	0.31	-0.53	<.001***	0.12	.137	-0.09	.279	-0.04	.850

Note. *** $p_{fdr} < 001$. ** $p_{fdr} < .01$. * $p_{fdr} < .05$. Aβ = amyloid-β. BA = Brodmann area. CA = cornu ammonis. DG = dentate gyrus. ErC = entorhinal cortex. GMV = gray matter volume. HT = hippocampal tail. IPC = inferior parietal cortex. IsthCing = isthmus cingulate. ITC = inferior temporal cortex. IV = independent variable. LOC = lateral occipital cortex. lOFC = lateral orbitorfrontal cortex. mOFC = medial orbitorfrontal cortex. Sub = subiculum. TP = temporal pole. PCC = posterior cingulate cortex. PhC = parahippocampal cortex. Prec = Precuneus.

Table A6

Pr (objects) predicted by PET and sMRI measures in the CU Aβ- diagnostic group

IV	Model statistics				Coefficients							
					Age		Sex (female)		Years of education		IV	
	n (excl.)	*F*	*p*	$R^2_{adj.}$	β	p_{fdr}	β	p_{fdr}	β	p_{fdr}	β	p_{fdr}
Early Aβ ROI SUVr (SD)	54 (5)	16.99 (5, 49)	<.001***	0.55	-0.66	<.001***	0.15	.153	-0.17	.114	0.15	.343
Braak I/II tau SUVr (SD)	57 (3)	21.71 (5, 52)	<.001***	0.60	-0.60	<.001***	0.17	.077	-0.26	.004**	-0.19	.116
CA1 $GMV_{adj.}$ (mm^3)	57 (3)	20.32 (5, 52)	<.001***	0.58	-0.65	<.001***	0.14	.129	-0.25	.006**	0.12	.759
CA2/3 $GMV_{adj.}$ (mm^3)	56 (4)	19.12 (5, 51)	<.001***	0.57	-0.71	<.001***	0.11	.240	-0.24	.011*	0.00	.978
DG $GMV_{adj.}$ (mm^3)	57 (3)	19.67 (5, 52)	<.001***	0.57	-0.68	<.001***	0.14	.140	-0.26	.006**	0.06	.978
Sub $GMV_{adj.}$ (mm^3)	57 (3)	19.37 (5, 52)	<.001***	0.57	-0.69	<.001***	0.13	.165	-0.25	.007**	0.00	.978
HT $GMV_{adj.}$ (mm^3)	57 (3)	20.30 (5, 52)	<.001***	0.58	-0.71	<.001***	0.14	.150	-0.23	.015*	-0.11	.759
ErC thickness (mm)	56 (4)	18.51 (5, 51)	<.001***	0.56	-0.71	<.001***	0.10	.280	-0.24	.015*	0.02	.937
BA35 thickness (mm)	56 (4)	19.63 (5, 51)	<.001***	0.58	-0.66	<.001***	0.10	.308	-0.23	.015*	0.13	.918
BA36 thickness (mm)	55 (5)	19.97 (5, 50)	<.001***	0.58	-0.71	<.001***	0.11	.278	-0.25	.009**	0.09	.918
PhC thickness (mm)	55 (5)	21.48 (5, 50)	<.001***	0.60	-0.71	<.001***	0.09	.345	-0.22	.013*	0.07	.918
IPC thickness (mm)	56 (4)	18.16 (5, 51)	<.001***	0.56	-0.69	<.001***	0.16	.118	-0.23	.015*	-0.02	.937
IsthCing thickness (mm)	54 (6)	15.84 (5, 49)	<.001***	0.53	-0.71	<.001***	0.12	.258	-0.21	.040*	-0.05	.918
LOC thickness (mm)	57 (3)	19.51 (5, 52)	<.001***	0.57	-0.67	<.001***	0.14	.147	-0.24	.011*	0.05	.918
mOFC thickness (mm)	56 (4)	21.62 (5, 51)	<.001***	0.60	-0.72	<.001***	0.16	.075	-0.29	.002**	-0.07	.918
PCC thickness (mm)	57 (3)	19.75 (5, 52)	<.001***	0.57	-0.68	<.001***	0.14	.138	-0.25	.007**	0.07	.918
Prec thickness (mm)	113 (8)	13.63 (5, 108)	<.001***	0.31	-0.49	<.001***	0.11	.200	-0.07	.360	0.08	.686
ITC thickness (mm)	114 (7)	13.99 (5, 109)	<.001***	0.32	-0.54	<.001***	0.10	.256	-0.09	.253	-0.02	.900
lOFC thickness (mm)	115 (6)	13.26 (5, 110)	<.001***	0.30	-0.48	<.001***	0.13	.116	-0.09	.284	0.10	.538
TP thickness (mm)	114 (7)	13.98 (5, 109)	<.001***	0.31	-0.53	<.001***	0.12	.137	-0.09	.279	-0.04	.850

Note. *** p_{fdr} < 001. **p_{fdr} < .01. *p_{fdr} < .05. Aβ = amyloid-β. BA = Brodmann area. CA = cornu ammonis. DG = dentate gyrus. ErC = entorhinal cortex. GMV = gray matter volume. HT = hippocampal tail. IPC = inferior parietal cortex. IsthCing = isthmus cingulate. ITC = inferior temporal cortex. IV = independent variable. LOC = lateral occipital cortex. lOFC = lateral orbitorfrontal cortex. mOFC = medial orbitorfrontal cortex. Sub = subiculum. TP = temporal pole. PCC = posterior cingulate cortex. PhC = parahippocampal cortex. Prec = Precuneus.

Table A7

Pr (scenes) predicted by PET and sMRI measures in the CU Aβ- diagnostic group

IV	Model statistics				Coefficients							
					Age		Sex (female)		Years of education		IV	
	n (excl.)	*F*	*p*	$R^2_{adj.}$	β	p_{fdr}	β	p_{fdr}	β	p_{fdr}	β	p_{fdr}
Early Aβ ROI SUVr (SD)	55 (4)	8.77 (5, 50)	<.001***	0.37	-0.54	<.001***	0.13	.283	-0.16	.177	0.11	.373
Braak I/II tau SUVr (SD)	56 (4)	8.69 (5, 51)	<.001***	0.36	-0.54	<.001***	0.15	.217	-0.27	.018*	0.07	.559
CA1 $GMV_{adj.}$ (mm^3)	55 (5)	7.75 (5, 50)	<.001***	0.33	-0.48	.001**	0.11	.362	-0.19	.095	0.12	.881
CA2/3 $GMV_{adj.}$ (mm^3)	56 (4)	8.58 (5, 51)	<.001***	0.36	-0.53	<.001***	0.14	.254	-0.21	.061	0.01	.978
DG $GMV_{adj.}$ (mm^3)	55 (5)	6.66 (5, 50)	<.001***	0.30	-0.47	<.001***	0.13	.301	-0.26	.029*	0.04	.978
Sub $GMV_{adj.}$ (mm^3)	56 (4)	7.50 (5, 51)	<.001***	0.32	-0.37	.009**	0.10	.406	-0.23	.044*	0.25	.532
HT $GMV_{adj.}$ (mm^3)	56 (4)	6.11 (5, 51)	<.001***	0.27	-0.49	<.001***	0.09	.481	-0.24	.053	0.05	.978
ErC thickness (mm)	55 (5)	9.65 (5, 50)	<.001***	0.39	-0.53	<.001***	0.10	.423	-0.28	.016*	-0.25	.596
BA35 thickness (mm)	55 (5)	8.91 (5, 50)	<.001***	0.37	-0.53	<.001***	0.16	.181	-0.22	.051	0.00	.992
BA36 thickness (mm)	56 (4)	6.20 (5, 51)	<.001***	0.27	-0.52	<.001***	0.07	.586	-0.25	.046*	-0.08	.918
PhC thickness (mm)	56 (4)	8.64 (5, 51)	<.001***	0.36	-0.56	<.001***	0.14	.255	-0.21	.061	-0.05	.918
IPC thickness (mm)	56 (4)	7.94 (5, 51)	<.001***	0.34	-0.43	.012*	0.18	.160	-0.27	.019*	0.06	.918
IsthCing thickness (mm)	55 (5)	7.48 (5, 50)	<.001***	0.32	-0.54	<.001***	0.09	.472	-0.20	.084	0.05	.918
LOC thickness (mm)	54 (6)	13.57 (5, 49)	<.001***	0.49	-0.71	<.001***	0.13	.245	-0.31	.004**	-0.25	.596
mOFC thickness (mm)	55 (5)	7.47 (5, 50)	<.001***	0.32	-0.56	<.001***	0.09	.449	-0.21	.082	-0.05	.918
PCC thickness (mm)	56 (4)	6.24 (5, 51)	<.001***	0.28	-0.48	<.001***	0.09	.477	-0.22	.058	0.08	.918
Prec thickness (mm)	56 (4)	8.37 (5, 51)	<.001***	0.35	-0.55	<.001***	0.15	.247	-0.28	.014*	-0.14	.918
ITC thickness (mm)	56 (4)	8.72 (5, 51)	<.001***	0.36	-0.57	<.001***	0.13	.295	-0.22	.052	-0.07	.918
lOFC thickness (mm)	55 (5)	10.56 (5, 50)	<.001***	0.41	-0.56	<.001***	0.17	.156	-0.25	.024*	-0.06	.918
TP thickness (mm)	55 (5)	8.43 (5, 50)	<.001***	0.35	-0.63	<.001***	0.11	.386	-0.17	.127	-0.20	.918

Note. *** $p_{fdr} < 001$. ** $p_{fdr} < .01$. * $p_{fdr} < .05$. Aβ = amyloid-β. BA = Brodmann area. CA = cornu ammonis. DG = dentate gyrus. ErC = entorhinal cortex. GMV = gray matter volume. HT = hippocampal tail. IPC = inferior parietal cortex. IsthCing = isthmus cingulate. ITC = inferior temporal cortex. IV = independent variable. LOC = lateral occipital cortex. lOFC = lateral orbitorfrontal cortex. mOFC = medial orbitorfrontal cortex. Sub = subiculum. TP = temporal pole. PCC = posterior cingulate cortex. PhC = parahippocampal cortex. Prec = Precuneus.

Table A8

Br (objects) predicted by PET and sMRI measures in the CU Aβ- diagnostic group

IV	Model statistics				Coefficients							
					Age		Sex (female)		Years of education		IV	
	n (excl.)	*F*	*p*	$R^2_{adj.}$	β	p_{fdr}	β	p_{fdr}	β	p_{fdr}	β	p_{fdr}
Early Aβ ROI SUVr (SD)	55 (4)	1.60 (5, 50)	.190	0.04	0.22	.156	-0.12	.419	0.16	.268	0.01	.972
Braak I/II tau SUVr (SD)	56 (4)	1.68 (5, 51)	.168	0.05	0.24	.147	-0.12	.423	0.16	.232	-0.07	.769
CA1 $GMV_{adj.}$ (mm^3)	55 (5)	2.23 (5, 50)	.079	0.08	0.33	.064	-0.13	.406	0.15	.280	0.20	.520
CA2/3 $GMV_{adj.}$ (mm^3)	56 (4)	2.07 (5, 51)	.098	0.07	0.29	.078	-0.11	.462	0.17	.193	0.18	.520
DG $GMV_{adj.}$ (mm^3)	56 (4)	1.67 (5, 51)	.171	0.05	0.24	.150	-0.11	.502	0.16	.237	0.07	.939
Sub $GMV_{adj.}$ (mm^3)	56 (4)	2.06 (5, 51)	.099	0.07	0.31	.070	-0.11	.484	0.17	.205	0.19	.520
HT $GMV_{adj.}$ (mm^3)	56 (4)	1.98 (5, 51)	.111	0.07	0.25	.106	-0.12	.437	0.14	.317	0.16	.520
ErC thickness (mm)	56 (4)	1.63 (5, 51)	.182	0.04	0.21	.173	-0.13	.385	0.16	.265	-0.03	.998
BA35 thickness (mm)	55 (5)	2.17 (5, 50)	.086	0.08	0.07	.662	-0.10	.520	0.08	.570	-0.28	.971
BA36 thickness (mm)	55 (5)	1.90 (5, 50)	.126	0.06	0.21	.200	-0.16	.294	0.22	.130	0.09	.998
PhC thickness (mm)	56 (4)	1.62 (5, 51)	.185	0.04	0.21	.225	-0.13	.389	0.17	.210	0.00	.998
IPC thickness (mm)	56 (4)	1.62 (5, 51)	.183	0.04	0.23	.256	-0.12	.441	0.17	.213	0.03	.998
IsthCing thickness (mm)	56 (4)	1.86 (5, 51)	.132	0.06	0.19	.212	-0.12	.413	0.19	.173	-0.13	.998
LOC thickness (mm)	56 (4)	1.64 (5, 51)	.179	0.04	0.24	.191	-0.12	.471	0.18	.201	0.04	.998
mOFC thickness (mm)	56 (4)	1.62 (5, 51)	.183	0.04	0.20	.205	-0.13	.382	0.16	.241	-0.02	.998
PCC thickness (mm)	56 (4)	1.64 (5, 51)	.179	0.04	0.22	.161	-0.13	.408	0.17	.211	0.04	.998
Prec thickness (mm)	56 (4)	1.73 (5, 51)	.158	0.05	0.15	.422	-0.15	.322	0.16	.228	-0.10	.998
ITC thickness (mm)	56 (4)	1.62 (5, 51)	.183	0.04	0.22	.204	-0.13	.409	0.17	.206	0.03	.998
lOFC thickness (mm)	56 (4)	1.68 (5, 51)	.170	0.05	0.22	.150	-0.12	.444	0.19	.184	0.06	.998
TP thickness (mm)	56 (4)	2.12 (5, 51)	.091	0.08	0.12	.445	-0.12	.403	0.18	.173	-0.20	.971

Note. *** $p_{fdr} < 001$. ** $p_{fdr} < .01$. * $p_{fdr} < .05$. Aβ = amyloid-β. BA = Brodmann area. CA = cornu ammonis. DG = dentate gyrus. ErC = entorhinal cortex. GMV = gray matter volume. HT = hippocampal tail. IPC = inferior parietal cortex. IsthCing = isthmus cingulate. ITC = inferior temporal cortex. IV = independent variable. LOC = lateral occipital cortex. lOFC = lateral orbitorfrontal cortex. mOFC = medial orbitorfrontal cortex. Sub = subiculum. TP = temporal pole. PCC = posterior cingulate cortex. PhC = parahippocampal cortex. Prec = Precuneus.

Table A9

Br (scenes) predicted by PET and sMRI measures in the CU Aβ- diagnostic group

IV	Model statistics				Coefficients							
					Age		Sex (female)		Years of education		IV	
	n (excl.)	*F*	*p*	$R^2_{adj.}$	β	p_{fdr}	β	p_{fdr}	β	p_{fdr}	β	p_{fdr}
Early Aβ ROI SUVr (SD)	52 (7)	1.75 (5, 47)	.155	0.06	0.21	.166	-0.16	.305	0.16	.298	-0.01	.972
Braak I/II tau SUVr (SD)	55 (5)	0.88 (5, 50)	.484	-0.01	0.13	.461	-0.12	.452	0.15	.293	-0.05	.769
CA1 $GMV_{adj.}$ (mm^3)	55 (5)	0.86 (5, 50)	.495	-0.01	0.12	.517	-0.12	.460	0.15	.275	0.02	.981
CA2/3 $GMV_{adj.}$ (mm^3)	55 (5)	0.97 (5, 50)	.430	0.00	0.06	.721	-0.13	.419	0.16	.267	-0.10	.842
DG $GMV_{adj.}$ (mm^3)	55 (5)	0.87 (5, 50)	.487	-0.01	0.09	.604	-0.13	.410	0.16	.261	-0.04	.981
Sub $GMV_{adj.}$ (mm^3)	55 (5)	2.07 (5, 50)	.098	0.07	0.28	.101	-0.10	.494	0.14	.295	0.33	.374
HT $GMV_{adj.}$ (mm^3)	55 (5)	0.85 (5, 50)	.498	-0.01	0.11	.509	-0.12	.435	0.15	.291	0.00	.981
ErC thickness (mm)	55 (5)	0.99 (5, 50)	.423	0.00	0.11	.471	-0.12	.425	0.19	.208	0.10	.998
BA35 thickness (mm)	55 (5)	1.47 (5, 50)	.226	0.03	0.00	.976	-0.10	.534	0.12	.391	-0.23	.971
BA36 thickness (mm)	55 (5)	0.96 (5, 50)	.438	0.00	0.14	.398	-0.10	.522	0.18	.220	0.09	.998
PhC thickness (mm)	54 (6)	2.22 (5, 49)	.080	0.08	0.01	.970	-0.13	.382	0.22	.103	-0.27	.971
IPC thickness (mm)	55 (5)	0.86 (5, 50)	.495	-0.01	0.08	.689	-0.13	.428	0.16	.271	-0.03	.998
IsthCing thickness (mm)	55 (5)	0.86 (5, 50)	.497	-0.01	0.10	.512	-0.12	.441	0.16	.273	-0.01	.998
LOC thickness (mm)	55 (5)	0.89 (5, 50)	.478	-0.01	0.07	.701	-0.14	.392	0.15	.298	-0.06	.998
mOFC thickness (mm)	55 (5)	0.85 (5, 50)	.497	-0.01	0.10	.532	-0.12	.434	0.15	.303	-0.01	.998
PCC thickness (mm)	55 (5)	0.85 (5, 50)	.498	-0.01	0.11	.501	-0.12	.436	0.15	.275	0.00	.998
Prec thickness (mm)	55 (5)	0.90 (5, 50)	.473	-0.01	0.06	.733	-0.14	.395	0.15	.287	-0.07	.998
ITC thickness (mm)	55 (5)	0.97 (5, 50)	.434	0.00	0.05	.796	-0.14	.382	0.14	.327	-0.10	.998
lOFC thickness (mm)	55 (5)	0.92 (5, 50)	.460	-0.01	0.09	.570	-0.13	.399	0.14	.329	-0.07	.998
TP thickness (mm)	54 (6)	1.28 (5, 49)	.291	0.02	-0.01	.944	-0.07	.673	0.21	.139	-0.22	.971

Note. *** $p_{fdr} < 001$. ** $p_{fdr} < .01$. * $p_{fdr} < .05$. Aβ = amyloid-β. BA = Brodmann area. CA = cornu ammonis. DG = dentate gyrus. ErC = entorhinal cortex. GMV = gray matter volume. HT = hippocampal tail. IPC = inferior parietal cortex. IsthCing = isthmus cingulate. ITC = inferior temporal cortex. IV = independent variable. LOC = lateral occipital cortex. lOFC = lateral orbitorfrontal cortex. mOFC = medial orbitorfrontal cortex. Sub = subiculum. TP = temporal pole. PCC = posterior cingulate cortex. PhC = parahippocampal cortex. Prec = Precuneus.

Table A10

Pr (objects) predicted by PET and sMRI measures in the CU Aβ+ diagnostic group

IV	Model statistics				Coefficients							
					Age		Sex (female)		Years of education		IV	
	n (excl.)	*F*	*p*	$R^2_{adj.}$	β	p_{fdr}	β	p_{fdr}	β	p_{fdr}	β	p_{fdr}
Early Aβ ROI SUVr (SD)	38 (3)	3.51 (5, 33)	.017**	0.21	-0.31	.049*	0.16	.285	0.00	.985	-0.32	.082
Braak I/II tau SUVr (SD)	39 (2)	4.15 (5, 34)	.008**	0.25	-0.37	.016*	0.23	.122	-0.07	.631	-0.20	.347
CA1 $GMV_{adj.}$ (mm^3)	40 (1)	2.63 (5, 35)	.051	0.14	-0.36	.024*	0.23	.142	-0.04	.790	0.01	.946
CA2/3 $GMV_{adj.}$ (mm^3)	38 (3)	3.64 (5, 33)	.015**	0.22	-0.36	.023*	0.29	.058	-0.14	.337	0.06	.946
DG $GMV_{adj.}$ (mm^3)	39 (2)	2.97 (5, 34)	.033**	0.17	-0.38	.018*	0.30	.076	-0.09	.543	-0.16	.785
Sub $GMV_{adj.}$ (mm^3)	40 (1)	2.48 (5, 35)	.061	0.13	-0.36	.035*	0.18	.258	-0.04	.817	0.06	.946
HT $GMV_{adj.}$ (mm^3)	39 (2)	2.25 (5, 34)	.084	0.12	-0.24	.153	0.14	.383	-0.10	.541	0.21	.785
ErC thickness (mm)	39 (2)	1.91 (5, 34)	.131	0.09	-0.31	.065	0.19	.242	-0.14	.435	-0.13	.853
BA35 thickness (mm)	38 (3)	3.02 (5, 33)	.032**	0.18	-0.32	.067	0.30	.061	-0.15	.379	-0.01	.978
BA36 thickness (mm)	38 (3)	3.44 (5, 33)	.019**	0.21	-0.37	.019*	0.33	.040*	-0.11	.495	-0.13	.853
PhC thickness (mm)	39 (2)	5.08 (5, 34)	.003**	0.30	-0.50	.002**	0.28	.052	-0.19	.204	-0.29	.390
IPC thickness (mm)	40 (1)	3.11 (5, 35)	.027**	0.18	-0.32	.097	0.20	.179	-0.16	.279	0.11	.853
IsthCing thickness (mm)	39 (2)	2.27 (5, 34)	.082	0.12	-0.18	.345	0.27	.092	-0.11	.483	0.18	.810
LOC thickness (mm)	39 (2)	3.87 (5, 34)	.011**	0.23	-0.44	.012*	0.27	.076	-0.10	.490	-0.06	.948
mOFC thickness (mm)	40 (1)	3.17 (5, 35)	.025**	0.18	-0.33	.038*	0.21	.181	-0.03	.835	0.20	.666
PCC thickness (mm)	40 (1)	2.68 (5, 35)	.047**	0.15	-0.35	.032*	0.24	.122	-0.05	.750	0.06	.948
Prec thickness (mm)	40 (1)	2.66 (5, 35)	.049**	0.15	-0.35	.040*	0.24	.126	-0.04	.776	0.05	.951
ITC thickness (mm)	38 (3)	2.78 (5, 33)	.043**	0.16	-0.17	.357	0.29	.075	-0.01	.930	0.28	.484
lOFC thickness (mm)	39 (2)	2.89 (5, 34)	.036**	0.17	-0.19	.255	0.24	.124	-0.05	.736	0.28	.390
TP thickness (mm)	40 (1)	2.66 (5, 35)	.049**	0.15	-0.34	.047*	0.23	.142	-0.04	.767	0.05	.951

Note. *** $p_{fdr} < 001$. ** $p_{fdr} < .01$. * $p_{fdr} < .05$. Aβ = amyloid-β. BA = Brodmann area. CA = cornu ammonis. DG = dentate gyrus. ErC = entorhinal cortex. GMV = gray matter volume. HT = hippocampal tail. IPC = inferior parietal cortex. IsthCing = isthmus cingulate. ITC = inferior temporal cortex. IV = independent variable. LOC = lateral occipital cortex. lOFC = lateral orbitorfrontal cortex. mOFC = medial orbitorfrontal cortex. Sub = subiculum. TP = temporal pole. PCC = posterior cingulate cortex. PhC = parahippocampal cortex. Prec = Precuneus.

Table A11

Pr (scenes) predicted by PET and sMRI measures in the CU Aβ+ diagnostic group

IV	Model statistics				Coefficients							
					Age		Sex (female)		Years of education		IV	
	n (excl.)	*F*	*p*	$R^2_{adj.}$	β	p_{fdr}	β	p_{fdr}	β	p_{fdr}	β	p_{fdr}
Early Aβ ROI SUVr (SD)	39 (2)	3.98 (5, 34)	.009**	0.24	-0.55	<.001***	0.00	.977	-0.14	.342	0.21	.169
Braak I/II tau SUVr (SD)	39 (2)	3.59 (5, 34)	.015**	0.21	-0.55	.001**	0.00	.975	-0.14	.367	0.14	.362
CA1 $GMV_{adj.}$ (mm^3)	39 (2)	3.30 (5, 34)	.022**	0.19	-0.51	.002**	0.01	.974	-0.11	.476	-0.01	.946
CA2/3 $GMV_{adj.}$ (mm^3)	39 (2)	3.84 (5, 34)	.011**	0.23	-0.53	<.001***	0.00	.998	-0.12	.412	-0.18	.785
DG $GMV_{adj.}$ (mm^3)	39 (2)	3.31 (5, 34)	.022**	0.20	-0.52	.002**	0.01	.946	-0.11	.463	-0.03	.946
Sub $GMV_{adj.}$ (mm^3)	39 (2)	3.56 (5, 34)	.016**	0.21	-0.56	.001**	0.01	.922	-0.13	.379	-0.14	.785
HT $GMV_{adj.}$ (mm^3)	39 (2)	3.59 (5, 34)	.015**	0.21	-0.53	.001**	0.03	.820	-0.11	.454	-0.14	.785
ErC thickness (mm)	39 (2)	3.42 (5, 34)	.019**	0.20	-0.51	.002**	0.00	.994	-0.16	.357	-0.10	.853
BA35 thickness (mm)	39 (2)	3.46 (5, 34)	.018**	0.21	-0.53	.001**	0.00	.978	-0.15	.349	-0.11	.853
BA36 thickness (mm)	39 (2)	3.30 (5, 34)	.022**	0.20	-0.51	.002**	0.01	.962	-0.11	.481	-0.02	.978
PhC thickness (mm)	38 (3)	3.54 (5, 33)	.016**	0.22	-0.46	.006**	0.03	.838	-0.09	.562	0.14	.853
IPC thickness (mm)	38 (3)	4.16 (5, 33)	.008**	0.25	-0.30	.108	0.08	.591	-0.10	.473	0.32	.390
IsthCing thickness (mm)	38 (3)	3.29 (5, 33)	.022**	0.20	-0.49	.009**	0.04	.809	-0.15	.316	0.00	.978
LOC thickness (mm)	39 (2)	3.31 (5, 34)	.022**	0.20	-0.52	.003**	0.00	.999	-0.11	.476	-0.02	.978
mOFC thickness (mm)	38 (3)	5.98 (5, 33)	<.001***	0.35	-0.50	<.001***	-0.08	.585	-0.14	.290	0.36	.318
PCC thickness (mm)	39 (2)	3.31 (5, 34)	.022**	0.20	-0.51	.002**	0.01	.961	-0.11	.466	0.02	.978
Prec thickness (mm)	38 (3)	4.14 (5, 33)	.008**	0.25	-0.40	.016*	0.08	.595	-0.08	.601	0.27	.390
ITC thickness (mm)	38 (3)	3.55 (5, 33)	.016**	0.22	-0.60	.001**	0.03	.844	-0.06	.660	-0.19	.762
lOFC thickness (mm)	39 (2)	4.36 (5, 34)	.006**	0.26	-0.46	.004**	-0.01	.936	-0.07	.619	0.25	.390
TP thickness (mm)	39 (2)	3.44 (5, 34)	.018**	0.20	-0.47	.007**	-0.01	.973	-0.11	.471	0.10	.853

Note. *** $p_{fdr} < 001$. ** $p_{fdr} < .01$. * $p_{fdr} < .05$. Aβ = amyloid-β. BA = Brodmann area. CA = cornu ammonis. DG = dentate gyrus. ErC = entorhinal cortex. GMV = gray matter volume. HT = hippocampal tail. IPC = inferior parietal cortex. IsthCing = isthmus cingulate. ITC = inferior temporal cortex. IV = independent variable. LOC = lateral occipital cortex. lOFC = lateral orbitorfrontal cortex. mOFC = medial orbitorfrontal cortex. Sub = subiculum. TP = temporal pole. PCC = posterior cingulate cortex. PhC = parahippocampal cortex. Prec = Precuneus.

Table A12

Br (objects) predicted by PET and sMRI measures in the CU Aβ+ diagnostic group

IV	Model statistics				Coefficients							
					Age		Sex (female)		Years of education		IV	
	n (excl.)	*F*	*p*	$R^2_{adj.}$	β	p_{fdr}	β	p_{fdr}	β	p_{fdr}	β	p_{fdr}
Early Aβ ROI SUVr (SD)	40 (1)	0.99 (5, 35)	.425	0.00	0.19	.263	-0.22	.188	0.06	.723	-0.04	.867
Braak I/II tau SUVr (SD)	38 (3)	0.80 (5, 33)	.533	-0.02	0.18	.310	-0.07	.689	0.20	.236	-0.04	.822
CA1 $GMV_{adj.}$ (mm^3)	38 (3)	1.28 (5, 33)	.297	0.03	0.22	.196	-0.26	.133	0.07	.699	0.11	.843
CA2/3 $GMV_{adj.}$ (mm^3)	40 (1)	1.22 (5, 35)	.321	0.02	0.17	.315	-0.21	.199	0.04	.790	-0.15	.843
DG $GMV_{adj.}$ (mm^3)	39 (2)	1.67 (5, 34)	.180	0.07	0.21	.210	-0.32	.070	0.14	.399	0.27	.703
Sub $GMV_{adj.}$ (mm^3)	37 (4)	2.90 (5, 32)	.037**	0.17	0.39	.027*	-0.27	.094	-0.04	.790	0.40	.241
HT $GMV_{adj.}$ (mm^3)	36 (5)	0.64 (5, 31)	.640	-0.04	0.24	.182	-0.07	.714	0.09	.621	0.06	.925
ErC thickness (mm)	38 (3)	3.20 (5, 33)	.025**	0.19	0.12	.442	0.02	.919	0.54	.007**	0.55	.144
BA35 thickness (mm)	39 (2)	1.57 (5, 34)	.205	0.06	0.22	.184	-0.15	.343	0.26	.152	0.32	.371
BA36 thickness (mm)	39 (2)	1.77 (5, 34)	.157	0.08	0.21	.205	-0.28	.094	-0.07	.701	-0.11	.685
PhC thickness (mm)	37 (4)	1.66 (5, 32)	.184	0.07	0.28	.119	-0.24	.146	0.14	.413	0.23	.428
IPC thickness (mm)	37 (4)	1.66 (5, 32)	.184	0.07	0.40	.059	-0.13	.452	-0.17	.299	0.31	.382
IsthCing thickness (mm)	39 (2)	1.73 (5, 34)	.166	0.07	0.26	.172	-0.29	.081	-0.03	.863	0.09	.693
LOC thickness (mm)	40 (1)	1.04 (5, 35)	.400	0.00	0.22	.233	-0.21	.222	0.05	.745	0.08	.693
mOFC thickness (mm)	38 (3)	1.44 (5, 33)	.244	0.04	0.19	.262	-0.23	.189	0.03	.868	-0.10	.690
PCC thickness (mm)	39 (2)	1.76 (5, 34)	.159	0.07	0.19	.254	-0.32	.052	-0.02	.894	-0.10	.685
Prec thickness (mm)	38 (3)	1.73 (5, 33)	.167	0.07	0.27	.128	-0.25	.133	-0.06	.691	0.19	.440
ITC thickness (mm)	40 (1)	1.95 (5, 35)	.125	0.09	0.36	.057	-0.17	.277	0.07	.646	0.33	.371
lOFC thickness (mm)	35 (6)	1.95 (5, 30)	.128	0.10	0.18	.311	-0.23	.183	0.03	.876	-0.25	.428
TP thickness (mm)	39 (2)	2.51 (5, 34)	.060	0.14	0.33	.058	-0.33	.042*	-0.02	.901	0.28	.371

Note. *** $p_{fdr} < 001$. ** $p_{fdr} < .01$. * $p_{fdr} < .05$. Aβ = amyloid-β. BA = Brodmann area. CA = cornu ammonis. DG = dentate gyrus. ErC = entorhinal cortex. GMV = gray matter volume. HT = hippocampal tail. IPC = inferior parietal cortex. IsthCing = isthmus cingulate. ITC = inferior temporal cortex. IV = independent variable. LOC = lateral occipital cortex. lOFC = lateral orbitorfrontal cortex. mOFC = medial orbitorfrontal cortex. Sub = subiculum. TP = temporal pole. PCC = posterior cingulate cortex. PhC = parahippocampal cortex. Prec = Precuneus.

Table A13

Br (scenes) predicted by PET and sMRI measures in the CU Aβ+ diagnostic group

IV	Model statistics				Coefficients							
					Age		Sex (female)		Years of education		IV	
	n (excl.)	*F*	*p*	$R^2_{adj.}$	β	p_{fdr}	β	p_{fdr}	β	p_{fdr}	β	p_{fdr}
Early Aβ ROI SUVr (SD)	38 (3)	1.36 (5, 33)	.269	0.04	0.21	.219	-0.02	.891	0.28	.094	0.03	.867
Braak I/II tau SUVr (SD)	37 (4)	1.67 (5, 32)	.180	0.07	0.29	.108	-0.04	.818	0.33	.055	-0.21	.523
CA1 $GMV_{adj.}$ (mm^3)	37 (4)	1.72 (5, 32)	.169	0.07	0.25	.140	-0.09	.607	0.20	.235	-0.14	.843
CA2/3 $GMV_{adj.}$ (mm^3)	38 (3)	1.40 (5, 33)	.255	0.04	0.21	.218	-0.02	.904	0.28	.092	-0.07	.925
DG $GMV_{adj.}$ (mm^3)	38 (3)	1.35 (5, 33)	.272	0.04	0.21	.203	-0.02	.904	0.28	.091	-0.01	.954
Sub $GMV_{adj.}$ (mm^3)	36 (5)	1.98 (5, 31)	.122	0.10	0.39	.041*	-0.15	.355	0.20	.222	0.23	.725
HT $GMV_{adj.}$ (mm^3)	38 (3)	1.35 (5, 33)	.271	0.04	0.21	.212	-0.02	.920	0.28	.090	-0.02	.954
ErC thickness (mm)	38 (3)	2.91 (5, 33)	.036**	0.17	0.18	.251	0.00	.988	0.53	.007**	0.42	.353
BA35 thickness (mm)	39 (2)	1.23 (5, 34)	.316	0.02	0.23	.171	-0.12	.464	0.27	.152	0.16	.562
BA36 thickness (mm)	38 (3)	1.40 (5, 33)	.254	0.04	0.22	.191	-0.06	.759	0.32	.090	0.09	.698
PhC thickness (mm)	36 (5)	1.93 (5, 31)	.130	0.10	0.31	.084	-0.10	.555	0.33	.065	0.21	.440
IPC thickness (mm)	37 (4)	1.93 (5, 32)	.130	0.09	0.40	.054	-0.08	.621	0.20	.224	0.22	.440
IsthCing thickness (mm)	37 (4)	2.20 (5, 32)	.092	0.12	0.42	.035*	-0.06	.740	0.21	.183	0.28	.382
LOC thickness (mm)	37 (4)	3.02 (5, 32)	.032**	0.18	0.43	.021*	0.00	.999	0.34	.034*	0.35	.371
mOFC thickness (mm)	37 (4)	2.01 (5, 32)	.116	0.10	0.20	.250	-0.06	.699	0.21	.193	-0.22	.428
PCC thickness (mm)	37 (4)	1.58 (5, 32)	.205	0.06	0.28	.109	-0.10	.549	0.22	.180	0.06	.720
Prec thickness (mm)	37 (4)	2.46 (5, 32)	.065	0.14	0.38	.033*	-0.05	.765	0.22	.176	0.30	.371
ITC thickness (mm)	38 (3)	2.08 (5, 33)	.105	0.10	0.37	.054	0.01	.972	0.29	.074	0.29	.382
lOFC thickness (mm)	38 (3)	1.52 (5, 33)	.220	0.05	0.26	.144	-0.05	.750	0.31	.069	0.14	.622
TP thickness (mm)	37 (4)	1.86 (5, 32)	.141	0.09	0.35	.062	-0.13	.425	0.22	.187	0.19	.461

Note. *** $p_{fdr} < 001$. ** $p_{fdr} < .01$. * $p_{fdr} < .05$. Aβ = amyloid-β. BA = Brodmann area. CA = cornu ammonis. DG = dentate gyrus. ErC = entorhinal cortex. GMV = gray matter volume. HT = hippocampal tail. IPC = inferior parietal cortex. IsthCing = isthmus cingulate. ITC = inferior temporal cortex. IV = independent variable. LOC = lateral occipital cortex. lOFC = lateral orbitorfrontal cortex. mOFC = medial orbitorfrontal cortex. Sub = subiculum. TP = temporal pole. PCC = posterior cingulate cortex. PhC = parahippocampal cortex. Prec = Precuneus.

Table A14

Pr (objects) predicted by PET and sMRI measures in the MCI Aβ+ diagnostic group

IV	Model statistics				Coefficients							
					Age		Sex (female)		Years of education		IV	
	n (excl.)	*F*	*p*	$R^2_{adj.}$	β	p_{fdr}	β	p_{fdr}	β	p_{fdr}	β	p_{fdr}
Early Aβ ROI SUVr (SD)	19 (1)	2.85 (5, 14)	.064	0.29	-0.23	.333	0.50	.060	0.35	.127	0.24	.574
Braak I/II tau SUVr (SD)	19 (1)	2.43 (5, 14)	.097	0.24	-0.12	.618	0.58	.030*	0.27	.267	-0.10	.724
CA1 $GMV_{adj.}$ (mm^3)	17 (3)	1.96 (5, 12)	.165	0.19	-0.10	.704	0.62	.075	0.20	.505	0.02	.953
CA2/3 $GMV_{adj.}$ (mm^3)	19 (1)	2.55 (5, 14)	.086	0.26	-0.17	.478	0.58	.030*	0.35	.145	0.15	.616
DG $GMV_{adj.}$ (mm^3)	19 (1)	2.69 (5, 14)	.075	0.27	-0.03	.899	0.64	.020*	0.29	.194	-0.21	.586
Sub $GMV_{adj.}$ (mm^3)	19 (1)	3.38 (5, 14)	.039**	0.35	-0.04	.863	0.54	.032*	0.44	.066	0.36	.341
HT $GMV_{adj.}$ (mm^3)	19 (1)	2.35 (5, 14)	.105	0.23	-0.16	.514	0.57	.034*	0.31	.184	-0.04	.953
ErC thickness (mm)	17 (3)	3.32 (5, 12)	.047**	0.37	-0.28	.278	0.36	.268	0.12	.601	0.33	.516
BA35 thickness (mm)	18 (2)	2.78 (5, 13)	.072	0.30	-0.15	.519	0.47	.089	0.48	.071	0.31	.516
BA36 thickness (mm)	18 (2)	3.07 (5, 13)	.055	0.33	-0.29	.244	0.56	.031*	0.37	.117	-0.04	.874
PhC thickness (mm)	19 (1)	2.48 (5, 14)	.092	0.25	-0.17	.467	0.61	.026*	0.30	.184	-0.13	.798
IPC thickness (mm)	18 (2)	3.35 (5, 13)	.043**	0.36	0.05	.849	0.52	.041*	0.36	.108	0.38	.452
IsthCing thickness (mm)	19 (1)	2.48 (5, 14)	.092	0.25	-0.11	.641	0.54	.050*	0.28	.221	0.13	.798
LOC thickness (mm)	18 (2)	1.85 (5, 13)	.180	0.17	-0.02	.951	0.52	.059	0.33	.181	0.13	.798
mOFC thickness (mm)	18 (2)	4.14 (5, 13)	.022**	0.43	-0.16	.444	0.39	.113	0.42	.049*	0.43	.404
PCC thickness (mm)	18 (2)	2.94 (5, 13)	.062	0.31	-0.16	.488	0.45	.089	0.34	.130	0.27	.516
Prec thickness (mm)	19 (1)	2.39 (5, 14)	.100	0.24	-0.16	.493	0.64	.045*	0.34	.181	-0.10	.798
ITC thickness (mm)	17 (3)	3.60 (5, 12)	.038**	0.39	-0.09	.675	0.49	.041*	0.46	.046*	0.38	.452
lOFC thickness (mm)	18 (2)	2.83 (5, 13)	.069	0.30	-0.13	.577	0.59	.026*	0.41	.085	0.27	.516
TP thickness (mm)	19 (1)	3.99 (5, 14)	.023**	0.40	-0.12	.577	0.56	.022*	0.42	.058	0.39	.404

Note. *** $p_{fdr} < 001$. ** $p_{fdr} < .01$. * $p_{fdr} < .05$. Aβ = amyloid-β. BA = Brodmann area. CA = cornu ammonis. DG = dentate gyrus. ErC = entorhinal cortex. GMV = gray matter volume. HT = hippocampal tail. IPC = inferior parietal cortex. IsthCing = isthmus cingulate. ITC = inferior temporal cortex. IV = independent variable. LOC = lateral occipital cortex. lOFC = lateral orbitorfrontal cortex. mOFC = medial orbitorfrontal cortex. Sub = subiculum. TP = temporal pole. PCC = posterior cingulate cortex. PhC = parahippocampal cortex. Prec = Precuneus.

Table A15

Pr (scenes) predicted by PET and sMRI measures in the MCI Aβ+ diagnostic group

IV	Model statistics				Coefficients							
					Age		Sex (female)		Years of education		IV	
	n (excl.)	*F*	*p*	$R^2_{adj.}$	β	p_{fdr}	β	p_{fdr}	β	p_{fdr}	β	p_{fdr}
Early Aβ ROI SUVr (SD)	17 (3)	5.40 (5, 12)	.010**	0.52	-0.22	.269	0.76	.004**	0.64	.008**	0.08	.687
Braak I/II tau SUVr (SD)	17 (3)	5.37 (5, 12)	.010**	0.52	-0.21	.285	0.79	.002**	0.65	.007**	0.06	.724
CA1 $GMV_{adj.}$ (mm^3)	17 (3)	6.27 (5, 12)	.006**	0.57	-0.18	.344	0.79	.001**	0.74	.004**	0.23	.507
CA2/3 $GMV_{adj.}$ (mm^3)	18 (2)	5.43 (5, 13)	.009**	0.51	-0.26	.189	0.48	.037*	0.24	.255	-0.42	.137
DG $GMV_{adj.}$ (mm^3)	18 (2)	13.81 (5, 13)	<.001***	0.75	-0.64	.002**	0.65	<.001***	0.78	<.001***	0.47	.113
Sub $GMV_{adj.}$ (mm^3)	17 (3)	9.01 (5, 12)	.001**	0.67	-0.04	.843	0.74	.001**	0.73	.001**	0.42	.137
HT $GMV_{adj.}$ (mm^3)	18 (2)	7.54 (5, 13)	.002**	0.61	-0.28	.120	0.73	.001**	0.64	.003**	0.14	.586
ErC thickness (mm)	17 (3)	8.64 (5, 12)	.002**	0.66	-0.20	.232	0.62	.007**	0.61	.004**	0.37	.404
BA35 thickness (mm)	17 (3)	7.85 (5, 12)	.002**	0.63	-0.22	.205	0.72	.002**	0.74	.002**	0.33	.404
BA36 thickness (mm)	16 (4)	6.54 (5, 11)	.006**	0.60	-0.13	.486	0.86	.001**	0.80	.003**	0.27	.516
PhC thickness (mm)	16 (4)	5.08 (5, 11)	.014**	0.52	-0.18	.401	0.70	.021*	0.61	.021*	0.25	.516
IPC thickness (mm)	18 (2)	7.17 (5, 13)	.003**	0.59	-0.30	.101	0.70	.002**	0.66	.002**	0.08	.798
IsthCing thickness (mm)	18 (2)	6.99 (5, 13)	.003**	0.59	-0.32	.084	0.69	.003**	0.65	.003**	0.03	.874
LOC thickness (mm)	18 (2)	7.12 (5, 13)	.003**	0.59	-0.31	.082	0.70	.002**	0.66	.002**	0.07	.798
mOFC thickness (mm)	17 (3)	5.49 (5, 12)	.009**	0.53	-0.22	.258	0.83	.002**	0.66	.007**	-0.10	.798
PCC thickness (mm)	19 (1)	3.90 (5, 14)	.025**	0.39	-0.20	.333	0.53	.033*	0.45	.041*	0.17	.710
Prec thickness (mm)	18 (2)	7.24 (5, 13)	.003**	0.59	-0.33	.064	0.76	.003**	0.69	.003**	-0.11	.798
ITC thickness (mm)	18 (2)	7.11 (5, 13)	.003**	0.59	-0.31	.096	0.70	.002**	0.66	.002**	0.07	.798
lOFC thickness (mm)	16 (4)	10.89 (5, 11)	<.001***	0.73	-0.20	.201	0.71	<.001***	0.85	<.001***	0.36	.404
TP thickness (mm)	17 (3)	6.55 (5, 12)	.005**	0.58	-0.39	.042*	0.69	.005**	0.65	.012*	0.07	.798

Note. *** $p_{fdr} < 001$. ** $p_{fdr} < .01$. * $p_{fdr} < .05$. Aβ = amyloid-β. BA = Brodmann area. CA = cornu ammonis. DG = dentate gyrus. ErC = entorhinal cortex. GMV = gray matter volume. HT = hippocampal tail. IPC = inferior parietal cortex. IsthCing = isthmus cingulate. ITC = inferior temporal cortex. IV = independent variable. LOC = lateral occipital cortex. lOFC = lateral orbitorfrontal cortex. mOFC = medial orbitorfrontal cortex. Sub = subiculum. TP = temporal pole. PCC = posterior cingulate cortex. PhC = parahippocampal cortex. Prec = Precuneus.

Table A16

Br (objects) predicted by PET and sMRI measures in the MCI Aβ+ diagnostic group

IV	Model statistics				Coefficients							
					Age		Sex (female)		Years of education		IV	
	n (excl.)	*F*	*p*	$R^2_{adj.}$	β	p_{fdr}	β	p_{fdr}	β	p_{fdr}	β	p_{fdr}
Early Aβ ROI SUVr (SD)	18 (2)	1.02 (5, 13)	.434	0.00	-0.25	.352	-0.36	.208	-0.08	.784	-0.42	.405
Braak I/II tau SUVr (SD)	19 (1)	0.62 (5, 14)	.659	-0.09	-0.31	.256	-0.17	.564	0.25	.406	0.16	.854
CA1 $GMV_{adj.}$ (mm^3)	19 (1)	1.58 (5, 14)	.234	0.11	-0.52	.042*	-0.11	.637	-0.20	.437	-0.39	.253
CA2/3 $GMV_{adj.}$ (mm^3)	18 (2)	0.92 (5, 13)	.481	-0.02	-0.40	.165	-0.30	.288	0.29	.282	0.10	.713
DG $GMV_{adj.}$ (mm^3)	18 (2)	0.60 (5, 13)	.670	-0.10	0.01	.983	-0.25	.364	-0.02	.942	-0.30	.493
Sub $GMV_{adj.}$ (mm^3)	19 (1)	2.25 (5, 14)	.116	0.22	-0.48	.058	-0.12	.593	-0.05	.839	-0.61	.121
HT $GMV_{adj.}$ (mm^3)	18 (2)	2.03 (5, 13)	.149	0.20	-0.72	.017*	-0.31	.222	-0.04	.857	-0.48	.157
ErC thickness (mm)	20 (0)	0.62 (5, 15)	.657	-0.09	-0.37	.164	-0.22	.411	0.01	.956	-0.06	.890
BA35 thickness (mm)	20 (0)	0.67 (5, 15)	.624	-0.08	-0.36	.167	-0.22	.385	-0.03	.909	-0.13	.880
BA36 thickness (mm)	19 (1)	0.56 (5, 14)	.692	-0.11	-0.28	.306	-0.24	.382	0.20	.469	0.08	.880
PhC thickness (mm)	20 (0)	0.74 (5, 15)	.581	-0.06	-0.33	.214	-0.28	.292	0.03	.908	0.17	.879
IPC thickness (mm)	20 (0)	0.74 (5, 15)	.578	-0.06	-0.44	.124	-0.24	.354	0.02	.930	-0.18	.879
IsthCing thickness (mm)	18 (2)	1.03 (5, 13)	.430	0.01	-0.51	.090	-0.13	.626	0.10	.679	-0.30	.879
LOC thickness (mm)	16 (4)	0.90 (5, 11)	.498	-0.03	-0.28	.503	-0.36	.213	0.03	.916	0.14	.880
mOFC thickness (mm)	18 (2)	1.34 (5, 13)	.306	0.07	-0.48	.087	-0.40	.155	0.22	.366	-0.30	.879
PCC thickness (mm)	19 (1)	0.78 (5, 14)	.555	-0.05	-0.33	.215	-0.24	.363	0.17	.498	-0.22	.879
Prec thickness (mm)	17 (3)	0.84 (5, 12)	.525	-0.04	-0.39	.245	-0.34	.357	0.17	.583	0.10	.880
ITC thickness (mm)	18 (2)	2.86 (5, 13)	.067	0.30	-0.82	.006**	-0.29	.182	-0.03	.877	-0.56	.481
lOFC thickness (mm)	20 (0)	0.89 (5, 15)	.492	-0.02	-0.40	.121	-0.28	.274	-0.08	.767	-0.26	.879
TP thickness (mm)	18 (2)	0.67 (5, 13)	.625	-0.08	-0.33	.237	-0.21	.429	0.09	.733	-0.15	.880

Note. *** $p_{fdr} < 001$. ** $p_{fdr} < .01$. * $p_{fdr} < .05$. Aβ = amyloid-β. BA = Brodmann area. CA = cornu ammonis. DG = dentate gyrus. ErC = entorhinal cortex. GMV = gray matter volume. HT = hippocampal tail. IPC = inferior parietal cortex. IsthCing = isthmus cingulate. ITC = inferior temporal cortex. IV = independent variable. LOC = lateral occipital cortex. lOFC = lateral orbitorfrontal cortex. mOFC = medial orbitorfrontal cortex. Sub = subiculum. TP = temporal pole. PCC = posterior cingulate cortex. PhC = parahippocampal cortex. Prec = Precuneus.

Table A17

Br (scenes) predicted by PET and sMRI measures in the MCI Aβ+ diagnostic group

IV	Model statistics				Coefficients							
					Age		Sex (female)		Years of education		IV	
	n (excl.)	*F*	*p*	$R^2_{adj.}$	β	p_{fdr}	β	p_{fdr}	β	p_{fdr}	β	p_{fdr}
Early Aβ ROI SUVr (SD)	19 (1)	1.91 (5, 14)	.164	0.17	-0.44	.070	-0.42	.081	-0.27	.263	-0.17	.478
Braak I/II tau SUVr (SD)	19 (1)	1.73 (5, 14)	.200	0.14	-0.45	.071	-0.42	.107	-0.24	.359	-0.05	.854
CA1 $GMV_{adj.}$ (mm^3)	18 (2)	4.70 (5, 13)	.014**	0.47	-0.30	.134	-0.43	.042*	-0.58	.013*	-0.47	.121
CA2/3 $GMV_{adj.}$ (mm^3)	18 (2)	2.22 (5, 13)	.123	0.22	-0.58	.026*	-0.49	.058	-0.07	.749	0.13	.651
DG $GMV_{adj.}$ (mm^3)	18 (2)	4.48 (5, 13)	.017**	0.45	0.08	.745	-0.46	.029*	-0.55	.018*	-0.50	.121
Sub $GMV_{adj.}$ (mm^3)	18 (2)	4.14 (5, 13)	.022**	0.42	-0.77	.005**	-0.30	.160	-0.31	.134	-0.63	.121
HT $GMV_{adj.}$ (mm^3)	19 (1)	2.42 (5, 14)	.098	0.24	-0.56	.026*	-0.36	.114	-0.11	.636	-0.32	.273
ErC thickness (mm)	19 (1)	2.20 (5, 14)	.122	0.21	-0.46	.052	-0.34	.149	-0.26	.248	-0.25	.879
BA35 thickness (mm)	18 (2)	2.39 (5, 13)	.105	0.25	-0.54	.028*	-0.38	.107	-0.28	.250	0.01	.956
BA36 thickness (mm)	18 (2)	2.71 (5, 13)	.077	0.29	-0.53	.027*	-0.39	.087	-0.23	.306	0.19	.879
PhC thickness (mm)	19 (1)	1.97 (5, 14)	.154	0.18	-0.49	.047*	-0.36	.142	-0.24	.298	-0.19	.879
IPC thickness (mm)	18 (2)	3.37 (5, 13)	.042**	0.36	-0.33	.143	-0.56	.016*	-0.44	.054	-0.30	.855
IsthCing thickness (mm)	19 (1)	1.79 (5, 14)	.186	0.15	-0.51	.061	-0.36	.154	-0.19	.426	-0.13	.880
LOC thickness (mm)	18 (2)	2.64 (5, 13)	.082	0.28	-0.28	.235	-0.56	.022*	-0.43	.073	-0.16	.879
mOFC thickness (mm)	18 (2)	3.34 (5, 13)	.043**	0.36	-0.61	.014*	-0.57	.021*	-0.20	.341	-0.42	.481
PCC thickness (mm)	19 (1)	3.22 (5, 14)	.045**	0.33	-0.50	.027*	-0.41	.059	-0.20	.320	-0.39	.481
Prec thickness (mm)	19 (1)	1.78 (5, 14)	.189	0.15	-0.49	.058	-0.41	.094	-0.21	.360	-0.10	.880
ITC thickness (mm)	18 (2)	3.21 (5, 13)	.049**	0.34	-0.74	.009**	-0.46	.045*	-0.14	.494	-0.44	.481
lOFC thickness (mm)	18 (2)	2.43 (5, 13)	.100	0.25	-0.54	.027*	-0.41	.104	-0.31	.198	-0.08	.880
TP thickness (mm)	17 (3)	2.99 (5, 12)	.063	0.33	-0.31	.174	-0.50	.035*	-0.47	.068	-0.04	.890

Note. *** $p_{fdr} < 001$. ** $p_{fdr} < .01$. * $p_{fdr} < .05$. Aβ = amyloid-β. BA = Brodmann area. CA = cornu ammonis. DG = dentate gyrus. ErC = entorhinal cortex. GMV = gray matter volume. HT = hippocampal tail. IPC = inferior parietal cortex. IsthCing = isthmus cingulate. ITC = inferior temporal cortex. IV = independent variable. LOC = lateral occipital cortex. lOFC = lateral orbitorfrontal cortex. mOFC = medial orbitorfrontal cortex. Sub = subiculum. TP = temporal pole. PCC = posterior cingulate cortex. PhC = parahippocampal cortex. Prec = Precuneus.